

## Response to Comments of Reviewer #1

Referee comments are in black. Author responses are in blue.

**General comments:** This manuscript presents a study of the features of aerosols over the Tibetan Plateau (TP), including the distribution of AOD and Extinction Ångstrom exponent, the types and sources of aerosols. The utilization of sunphotometer measurements (CE318) is effective, which is significant to provide evidence of aerosol properties over the TP. However, some major revisions including content organization are needed. Moreover, improvement in English is needed before the paper can be accepted for publication. Therefore, I recommend publication after the authors address the following issues.

**Response:** We are very grateful for your important and constructive comments and suggestions. Some major revisions have been made carefully according to the comments and suggestions of this manuscript. Moreover, the grammar in the paper has been carefully checked and the language of this manuscript has been edited by native English speakers.

### **Major comments:**

1. The combination of case and long-term study, ground-based and satellite observation analysis together with the model simulation including two models need reorganized according to the scientific goal in this study.

**Response:** We have try our best to reorganize the content according to the reviewer's suggestion. Some large modifications and detail adjustments have been made in the revised version.

The content of section 3.1 is reorganized (the adjusted order is from monthly to seasonal and then to annual variations) and the titles of section 3.1 and 3.2 have been corrected as "*Aerosol properties observed by the CE318 instruments*" and "*Aerosol properties from MODIS*", respectively.

And, at the first of section 3.2, a statement of the relationship of ground-based to satellite observation ("*Ground-based observations can offer accurate aerosol optical properties at point locations but lack spatial coverage. The MODIS aerosol product can provide the spatial variation of AOD over the TP.*") has been added to connect the section 3.1 ground-based measurement and section 3.2 satellite observation.

In order to connect the case to the above, a transition has been added at the first of section 5. "*The aerosol long-range transport can cause the aerosol pollution and affect the long-term aerosol variation over the TP. In addition, the dominant aerosol type may change at the TP sites during a case of aerosol transport. Thus...*"

As for last paragraph of case analysis, the model simulation and HYSPLIT back trajectories have been combined with the ground and satellite observations to show the

1 aerosol transport and mixture over the TP.

2 2.The reliability of CE318 observation should be described in Section 2.2.1. Though  
3 the authors illustrated the errors, the situation of instrument calibration should be  
4 described here.

5 Response: In order to verify the accuracy and reliability, we have added the data  
6 retrieval references (“*Dubovik and King, 2000; Dubovik et al., 2006*”) and the  
7 instrument calibration in section 2.2.1, as followed:

8 *“The instruments were periodically calibrated using the Langley method at AERONET*  
9 *global calibration sites (the Izaña, Spain or the Mauna Loa, USA) or using the inter-*  
10 *comparison calibration method at the Beijing-CAMS site (Che et al., 2015). The cloud-*  
11 *screened and quality-controlled data of AOD, Extinction Ångstrom exponent (EAE),*  
12 *and aerosol volume size distribution ( $dV(r)/d\ln r$ ) are used in this work (Giles et al.,*  
13 *2019).”*

14  
15 3.What is the reason of “The CE318 observed AOD larger than 0.4 at each site is  
16 considered as the aerosol pollution over TP”? An appropriate reference is needed, or  
17 the background AOD should be provided.

18 Response: The figure 2 showed the annual mean values of AOD at 440nm at the five  
19 Tibetan Plateau sites are less than 0.14. Xia et al., (2015) and Cong et al., (2009) have  
20 showed the mean AODs observed by CE318 instruments at TP sites were less than 0.11.  
21 Thus, the value of 0.4 is larger than the three times the mean value at TP CE318  
22 sunphotometer sites. Besides, the value of 0.4 is normal regarded as high aerosol  
23 loading (Eck et al., 2010; Giles et al., 2012). According to this suggestion, the sentence  
24 has been changed and the reason is added as followed:

25 *“The CE318 observed AOD at 440 nm with values larger than 0.4 at each site was*  
26 *specially analysed to study the aerosol properties of the high aerosol loading over the*  
27 *TP. The value of 0.4 was selected because the mean annual values of AOD observed by*  
28 *CE318 instruments at the TP sites were less than ~0.1 in the past studies (Xia et al.,*  
29 *2016; Cong et al., 2009), and this value is normally regarded as the high aerosol*  
30 *loading (Eck et al., 2010; Giles et al., 2012)”*

31  
32 4.What is the role of GEOS-Chem model? According to the role of model, in the  
33 methodology, the details of model description should be shown separately.

34 Response: The GEOS-Chem model was used to simulate the aerosol variation during  
35 the case period. According to this suggestion, a separate paragraph of GEOS-Chem  
36 model description has been added as following:

37 *“The GEOS-Chem chemical transport model (version 11-01) coupled with the online*  
38 *radiative transfer calculations (RRTMG) at  $0.5^\circ \times 0.667^\circ$  horizontal resolution over*  
39 *the East Asia domain (Bey et al., 2001; Wang et al., 2004) was used. The model was*  
40 *driving by the Global Modeling and Assimilation Office (GMAO) MERRA-2*  
41 *meteorology with the temporal resolution of 3 hours for meteorological parameters and*  
42 *1 hour for surface fields. The simulation type of full chemistry in the troposphere was*  
43 *selected. The implementation of RRTMG in GEOS-Chem was described in Heald et al.*  
44 *(2014). The AOD was calculated according to Martin et al. (2003). The default global*

1 *anthropogenic emissions were overwritten over East Asia by the MIX inventory from Li*  
2 *et al. (2014). The Global Fire Emission Database (GFED) (van der Werf et al., 2010)*  
3 *has been used to specify emissions from fire. More details on the model and the other*  
4 *emissions data used and the evaluation of AOD in the east and south of the TP were*  
5 *shown in Zhu et al. (2017)”*

6  
7 5. In Section 3.1, the wavelength of AOD analyzed here should be given. Moreover, the  
8 authors analyzed the trend of AOD in Section 3.1, a significance check is needed.

9 Response: Thanks the reviewer’s comments. We have added the wavelength description  
10 of this manuscript in section 2.3, i.e., *“In this study, the AOD from the CE318, MODIS,*  
11 *and GEOS-Chem model were used. For convenience, CE318\_AOD, MODIS\_AOD, and*  
12 *Model\_AOD stand for the AOD observed by CE318, MODIS, and the AOD simulated*  
13 *by the GEOS-Chem model, respectively. For CE318\_AOD, the 440 nm wavelength is*  
14 *often studied, while MODIS\_AOD and Model\_AOD generally use the data at 550 nm*  
15 *wavelength. Thus, unless otherwise specified, CE318\_AOD, MODIS\_AOD, and*  
16 *Model\_AOD hereinafter represent the ones at 440 nm, 550 nm, and 550 nm,*  
17 *respectively.”*

18  
19 According to the reviewer comment, we have added the markers at the site which meet  
20 the 90% and 95% significances level in the corresponding figure. *“\* stands for 90%*  
21 *significance and \*\* represents 95% significance.”*

22  
23 6. What is the purpose of using CALIPSO observation data?

24 Response: The CALIPSO data were used to show the vertical feature of aerosol  
25 (including aerosol profile and aerosol type) during the case period. In revised version,  
26 the purpose of using CALIOP has been added in the third paragraph of section 2.3 with  
27 MODIS and HYSPLIT back trajectories as followed:

28 *“The HYSPLIT back trajectories, and the MODIS and CALIOP products were used to*  
29 *show the potential aerosol sources, spatial aerosol loading and the vertical features of*  
30 *the aerosol over the TP during the case period.”*

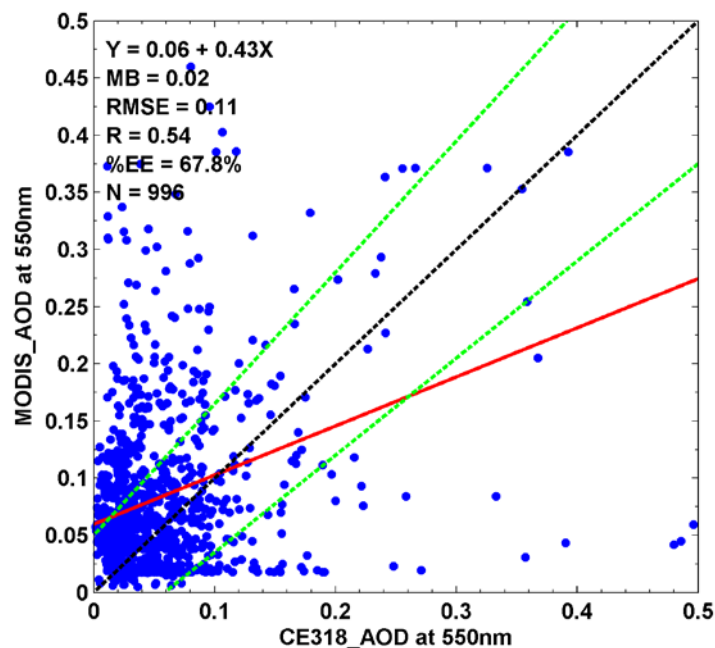
31  
32 7. What is the relationship between the ground-based and satellite observations? Since  
33 the authors have the valuable ground-based data, an evaluation of satellite observation,  
34 including MODIS and CALIPSO, can be performed, which is a good basis to get the  
35 spatial variation of aerosol properties in Section 3.2.

36 Response: Ground-based observation can offer more accurate aerosol optical properties  
37 at only one location (point) but lack spatial coverage. Satellite observation can make up  
38 for it. Hence, they are complementary. In the section 2.2, we had introduced some  
39 references about the evaluations of the satellite data. The simple comparison of mean  
40 values between CE318 and MODIS was shown in figure 5 in the original version.  
41 According to the reviewers’ suggestion, we have added the comparison of  
42 MODIS\_AOD and CE318\_AOD in revised version at section 3.2 as followed:

43 *“Ground-based observations can offer accurate aerosol optical properties at point*  
44 *locations but lack spatial coverage. The MODIS aerosol product can provide the spatial*

1 variation in AOD over the TP. Thus, we evaluated the MODIS\_AOD using the ground-  
 2 based observation CE318\_AOD at 550 nm over the TP sites. The CE318\_AOD at 550  
 3 nm was interpolated from 440 nm, 675 nm, 870 nm and 1020 nm by using an established  
 4 fitting method from Ångström (1929). The matchup method was that the CE318 data  
 5 within 1 hour of the MODIS overpass were compared with the MODIS data within a 25  
 6 km radius of the ground-based site. The minimum requirement for a matchup was at  
 7 least 3 pixels from MODIS.

8  
 9 Figure 5 shows the results of MODIS\_AOD compared to the collocated ground CE318  
 10 observations over the TP. There are 996 instantaneous matchups of Terra and Aqua  
 11 MODIS during the CE318 instrument measurement period at the five TP sites. The  
 12 MODIS\_AOD overestimates the AOD at 550 nm with a positive mean bias of 0.02 and  
 13 a root mean squared error (RMSE) of 0.11. The RMSE value is lower than that of the  
 14 North China Plain sites (~0.25) (Bilal et al., 2019). The slope and intercept of the best-  
 15 fit equation between the MODIS\_AOD and CE318\_AOD at 550 nm are 0.46 and 0.06,  
 16 respectively, with a correlation coefficient (R) of 0.54. There are 67.8% of the compared  
 17 AODs within the expected error envelope of  $0.05+0.15AOD$  (%EE). The R value is  
 18 lower than that in the global assessment statistics, while the %EE is higher than that in  
 19 the global evaluation (Bilal and Qiu, 2018). Overall, the results suggest that the  
 20 MODIS\_AOD product can be used to study the aerosol spatial variation over the TP  
 21 region.



22  
 23 Figure 5. Comparisons of the 550 nm AOD measured by the CE318 instrument  
 24 (CE318\_AOD) over Tibetan Plateau stations with the MODIS retrieval Deep-  
 25 Blue/Dark-Target combined AOD of 10 km spatial resolutions (MODIS\_AOD). The  
 26 statistical parameters in this figure include the number of matchup data (N), the slope  
 27 and intercept at the y-axis of linear regression (read line), the mean bias (MB), root  
 28 mean squared error (RMSE), correlation coefficient (R), and the percentage of data

1 *within the expected error  $0.05+0.15AOD$  (%EE) which is used as the MODIS AOD*  
2 *expected uncertainty over land (green lines)."*

3 In this study, MODIS AOD was used to show the spatial variation which can cover the  
4 shortage of CE318 sunphotometer observations. But CALISPO data were only used to  
5 show the vertical feature of aerosol during the case period. Thus, we have added the  
6 evaluation reference of CALIPSO data in section 2.3 as followed:

7 *"Kumar et al. (2018) have showed that the AOD from CALIOP version 4.10 agreed*  
8 *with the ground-based CE318 observation at a site in the central Himalayas with a*  
9 *correlation > 0.9 and ~ 87 % matchup data were within the expected error."*

10  
11 8. Page 5 Line 43 and 44, the authors think the positive trend of AOD and EAE at most  
12 sites over TP is caused by the addition of fine mode aerosol mainly from the  
13 anthropogenic impact. However, dust aerosols transported to the TP over long distances  
14 also has a small particle radius, causing similar changes. Thus, the authors should also  
15 take it into consideration.

16 *Response: Agree with this comment. This sentence has been change as "Looking at the*  
17 *CE318\_AOD and EAE values together, the positive trend of CE318\_AOD and the*  
18 *positive trend of EAE in the long term variation at most sites over TP indicates the*  
19 *addition of fine mode aerosol which may be related to the anthropogenic impact or*  
20 *long-distance transport of dust to the TP."*

21  
22 9. Figure 3 contains a lot of information, the authors need to indicate whether the values  
23 in the paper are the average, median or otherwise.

24 *Response: Thanks for the comments. The values used in the paper are the averages,*  
25 *including monthly, seasonal and annual averages. We have added the statement of*  
26 *monthly and annual means (averages) in the figure caption ("The asterisk symbols*  
27 *indicate the geometric means in each month. The annual mean values and standard*  
28 *errors are also shown in each subgraph.") and the corresponding text, such as*  
29 *"However, the monthly mean CE318\_AOD at Mt\_WLG is nearly symmetrical..." in*  
30 *second paragraph in section 3.1 and "This size distribution explained the relatively low*  
31 *annual averages of EAE..." at the fourth paragraph in section 3.1 in the revised version.*  
32

33 10. The authors mainly consider the anthropogenic aerosols in Southeast Asia, however,  
34 according to some research (e.g., Jia et al., AE, 2015), dust storm also occurs in the  
35 Indian peninsula. Can the authors separately estimate the contribution of anthropogenic  
36 aerosol and dust aerosol transported to the TP from Southeast Asia? Can the GEOS-  
37 Chem gives such evidence?

38 *Response: According the reviewer's comments, we have made some modification at*  
39 *the related content. The fourth paragraph of section 5, "High values in South Asia was*  
40 *caused by biomass burning, while..." has been corrected as "The high values in South*  
41 *Asia were caused by anthropogenic aerosols (such as biomass burning) or dust polluted*  
42 *by anthropogenic aerosols...". Besides, in the last paragraph of section 5, this reference*  
43 *has been added and discussed in this case, as followed:*

44 *"Jia et al. (2015) has shown that the dust from India polluted by anthropogenic aerosols*

1 can be transported to the TP, but the back trajectories on 1 and 3 May illustrated that  
2 the airflows that ended at Lhasa were from the north or northwest rather than the south,  
3 indicating that the polluted dust over the TP on 3 May was more likely the mixing result  
4 of dust and smoke aerosol. In addition, the lengths of the back trajectories (especially  
5 the back trajectories at 10 m and 500 m above ground level) on 1 May showed that the  
6 airflows moved slowly, which allowed the possibility of aerosol mixture over the TP.”

7  
8 According to Jia et al. (2015), the dust from India transported to TP is mainly occurred  
9 in west region of TP and much less than that from Taklimakan Desert. In addition, the  
10 dust from India is generally polluted by anthropogenic aerosols (Jia et al., 2015). Theory,  
11 GEOS-Chem model can give the contributions of anthropogenic aerosol and dust  
12 aerosol through multi-group sensitivity experiments of controlling the related emission  
13 inventories in the research region. But, the results may be not reliable (especially for  
14 TP region) for the inventories and the chemical, mixing, aging, deposition processes  
15 and so on. And the evaluations of the model results need more measurement  
16 experiments and chemical observed data which are hard to obtain. This is not the goal  
17 of this manuscript. This question is worthwhile to study in the next step.

18  
19 **Minor comments:**

20 1. Page 3, Line 9-10, what is the meaning of “large scale”? Spatial scale or temporal  
21 scale? The sentence need be illustrated clearly.

22 *Response: It has been corrected as “large spatial scale”.*

23  
24 2. Page 3 Line 10, “satellite remote sensing method (Li et.” should be “satellite remote-  
25 sensing method (Li et.”, in which a space is needed between “method” and “(”. In the  
26 whole manuscript, such writing problem should be paid attention, for example, Page 3,  
27 Line 20, there should be a space between “2007;” and “Xia”, etc.

28 *Response: All of them has been corrected.*

29  
30 3. Page 3, Line 27, there is mistake in grammar in sentence “there is an urgent need  
31 to. . . .”.

32 *Response: It has been corrected as “it is very essential to...”.*

33  
34 4. Page 4, Line 3, “2.1 site” should be “2.1 Site”.

35 *Response: Corrected.*

36  
37 5. Page 4, Line 6, there is mistake in grammar in sentence “site where can  
38 suffer from the local anthropogenic emissions”.

39 *Response: It has been corrected as “site that suffers from the local anthropogenic  
40 emissions”.*

41  
42 6. Before the unit, there need a space, for example, Page 4, Line 34, “2330km”.

43 *Response: All of these have been corrected in revised version.*

- 1 7. Page 5 Line 41 and 42, 'Mt\_WLG sites' should be 'Mt\_WLG site'.
- 2 [Response: It has been corrected.](#)
- 3

1 **Marked-up Manuscript:**

## 2 **Spatiotemporal variation of aerosol and potential long-range** 3 **transport impact over Tibetan Plateau, China**

4 Jun Zhu<sup>1,2,3</sup>, Xiangao Xia<sup>2,4</sup>, Huizheng Che<sup>3</sup>, Jun Wang<sup>5</sup>, Zhiyuan Cong<sup>6</sup>, Tianliang  
5 Zhao<sup>1</sup>, Shichang Kang<sup>7,9</sup>, Xuelei Zhang<sup>8</sup>, Xingna Yu<sup>1</sup>, Yanlin Zhang<sup>1</sup>

7 <sup>1</sup> Collaborative Innovation Center on Forecast and Evaluation of Meteorological Disasters, Key  
8 Laboratory for Aerosol-Cloud-Precipitation of China Meteorological Administration, Nanjing  
9 University of Information Science and Technology, Nanjing 210044, China;

10 <sup>2</sup> LAGEO, Institute of Atmospheric Physics, Chinese Academy of Sciences, Beijing 100029, China;

11 <sup>3</sup> State Key Laboratory of Severe Weather (LASW) and Key Laboratory of Atmospheric Chemistry  
12 (LAC), Chinese Academy of Meteorological Sciences, CMA, Beijing, 100081, China;

13 <sup>4</sup> University of Chinese Academy of Sciences, Beijing, 100049, China;

14 <sup>5</sup> Center of Global and Regional Environmental Research and Department of Chemical and  
15 Biochemical Engineering, University of Iowa, Iowa City, Iowa, USA;

16 <sup>6</sup> Key Laboratory of Tibetan Environment Changes and Land Surface Processes, Institute of Tibetan  
17 Plateau Research, Chinese Academy of Sciences, Beijing 100101, China;

18 <sup>7</sup> State Key Laboratory of Cryospheric Science, Northwest Institute of Eco-Environment and  
19 Resources, Chinese Academy of Sciences, Lanzhou 730000, China;

20 <sup>8</sup> Northeast Institute of Geography and Agroecology, Chinese Academy of Sciences, Changchun  
21 130102, China;

22 <sup>9</sup> CAS Center for Excellence in Tibetan Plateau Earth Sciences, China.

24 Corresponding author: Jun Zhu ([junzhu@nuist.edu.cn](mailto:junzhu@nuist.edu.cn)) & Xiangao Xia ([xxa@mail.iap.ac.cn](mailto:xxa@mail.iap.ac.cn))

### 26 **Abstract:**

27 The long-term temporal-spatial variations ~~of in the~~ aerosol optical properties ~~in-over the~~ Tibetan  
28 Plateau (TP) and the potential long-range transport from surrounding areas to TP were ~~analyzed~~  
29 ~~analysed~~ in this work, by using multiple years of sunphotometer measurements (CE318) at five  
30 stations in ~~the~~ TP, satellite aerosol production~~s~~ from ~~the~~ Moderate Resolution Imaging  
31 Spectroradiometer (MODIS) and Cloud-Aerosol Lidar with Orthogonal Polarization (CALIOP),  
32 back-trajectory analysis from the Hybrid Single-Particle Lagrangian Integrated Trajectory  
33 (HYSPLIT) and model simulations ~~of-from~~ the Goddard Earth Observing System (GEOS)-Chem  
34 chemistry transport model. The results from ~~the~~ ground-based observations show that the annual  
35 aerosol optical depth (AOD) ~~at 440 nm~~ at most TP sites increased in ~~the-past~~recent decades with  
36 trends of  $0.001\pm 0.003/\text{year}$  at Lhasa,  $0.013\pm 0.003/\text{year}$  at Mt\_WLG,  $0.002\pm 0.002/\text{year}$  at NAM\_CO,  
37 and  $0.000\pm 0.002/\text{year}$  at QOMS\_CAS. The increasing trend ~~is-was~~ also found for the aerosol  
38 Extinction Ångström exponent (EAE) at most sites, ~~except for~~ ~~with the exception of the~~ Mt\_WLG  
39 sites ~~with-an-obvious-decreasing-trend~~. Spatially, the AOD ~~at 550 nm~~ observed from MODIS ~~shows~~  
40 ~~showed~~ negative trends ~~in-at~~ the northwest edge closed to the Taklimakan Desert and ~~to the~~ east of  
41 the Qaidam Basin and slightly positive trends in most of the other areas ~~of the~~ TP. Different aerosol  
42 types and sources contributed ~~to the-a~~ polluted day (with CE318 AOD at 440\_nm > 0.4) ~~in-at~~ the

1 five sites ~~of~~on the TP: dust was dominant aerosol type in Lhasa, Mt\_WLG and Muztagh with  
2 sources ~~from~~in the Taklimakan Desert but fine aerosol pollution was dominant at NAM\_CO and  
3 QOMS\_CAS with ~~the~~ transport from South Asia. A case of aerosol pollution at Lhasa, NAM\_CO  
4 and QOMS\_CAS during 28 April – 3 May 2016 ~~reveals~~revealed that the smoke aerosols ~~is~~from  
5 South Asia were lifted up to 10\_km and transported to the TP, while the dust from the Taklimakan  
6 Desert could climb the north slope of the TP and then be transported to the ~~center~~central TP. The  
7 long-range transport of aerosol thereby seriously impacted ed the aerosol loading over the TP.

8 **Keywords:** Aerosol optical depth, Tibetan Plateau, aerosol pollution, long-range transport

9  
10

## 1. Introduction

The heavy haze ~~that has~~ occurred in ~~past-recent~~ years in China ~~was-has been~~ largely attributed to the atmospheric aerosols (Zhang et al., 2015). ~~Besides~~In addition, atmospheric aerosols can affect the climate through the interactions between aerosol-radiation and between aerosol-cloud (Takemura et al., 2005; Li et al., 2017), while the clouds and its precipitation are also ~~in-connection with-the~~connected to large scale atmospheric circulations (Yang et al., 2010; Yang et al., 2017a). However, ~~there is still a high level of the~~uncertainty ~~of-about~~ the impact of aerosols on the climate ~~effect is still high~~, which is mostly due to the highly spatiotemporal variability of aerosols. Therefore, ~~the study of studying the-aerosol~~ physical and chemical properties of aerosols over different regions is ~~very~~ essential. ~~Ground-based measurements can offer more accuracy data of aerosol properties, while large-scale observation of aerosol optical and physical properties needs satellite remote-sensing method. Thus, long-term detection of aerosols from both of the ground and satellite platforms is absolutely necessary to improve understanding of the climate effects of aerosol.~~

The Tibetan Plateau (TP), is the largest elevated plateau in East Asia and considered as one of the most pristine terrestrial regions, ~~alongside-along with~~ the Arctic and Antarctic. However, in the past two decades, ~~the~~ TP has been surrounded by ~~the-an unprecedented-unprecedented~~ growing growth of emissions of Asian air pollutants from ~~the~~ various sources. Consequently, some ~~researches~~ studies have demonstrated that the aerosols transported from its around areas (South Asia and Taklimakan Desert) have polluted the TP (Huang et al., 2007; Xia et al., 2011; Kopacz et al., 2011; Lu et al., 2012; Liu et al., 2015). The increase in aerosols over the TP may have an important impact on the regional or global climate. Lau et al. (2006) has suggested that increased absorbing aerosols (dust and black carbon) over ~~the~~ TP may create a positive tropospheric temperature anomaly over ~~the~~ TP and adjacent regions to the south, causing the advance and enhancement of the Indian summer monsoon. ~~While-a~~ Attempts ~~were-have been~~ made to reveal the linkages between ~~the~~ climate change (such as changes to glaciers and monsoons) and the air pollutants around ~~the~~ TP (mainly absorbing carbonaceous materials) (Qian et al., 2011; Wang et al., 2016; Lee et al., 2013). ~~However~~, the quantitative effect of the TP aerosol on climate variability remains largely unknown, and ~~there is an urgent need~~ it is very essential to fully understand the aerosol characteristics over ~~the~~ TP.

A large amount of attention has been paid to aerosol characteristics over the TP (Wan et al., 2015; Tobo et al., 2007; Zhao et al., 2013; Liu et al., 2008; Du et al., 2015). Although the seasonal variations in aerosol properties over the TP have been analysed based on ground-based observations or satellite products (Shen et al., 2015; Xia et al., 2008), analysis is needed of the long-term trends in the variation of aerosols over the TP to provide predictions and guidelines for environment policies. In past studies, spring or summer have often been studied due to the important impacts of dust and carbonaceous aerosols (Huang et al., 2007; Cong et al., 2007; Lee et al., 2013). ~~However~~, most studies of the aerosol properties based on ground-based measurements have been conducted at a single site over the TP, such as NAM CO (Cong et al., 2009), Mt. Yulong (Zhang et al., 2012), and Mt. WLG (Che et al., 2011). ~~Past studies analyzing the aerosol variation in TP used ground-based observations and satellite products, but many of these~~ Past studies have mostly focused on ~~the~~ single stations or short-term variations due to the ~~difficulties~~ difficulty ~~to-of take-taking a~~ the sufficient number of ground-based observations in challenging weather conditions over the remote plateau.

1  
2 Ground-based measurements can offer more accurate data on aerosol properties, while large-  
3 scale spatial observations of aerosol optical and physical properties require satellite remote-sensing  
4 methods (Li et al., 2015; Li et al., 2018; Xing et al., 2017). Thus, the long-term detection of aerosols  
5 from both ground and satellite platforms is absolutely necessary for improving our understanding  
6 of the climate effects of aerosol over the TP region. Consequently, based on multiple years of  
7 observations from five ground-based sunphotometers at the TP and the MODIS aerosol optical depth  
8 product over the TP region, our work here is ~~to~~ focused on the long-term spatiotemporal-spatial  
9 variations of in the aerosol optical properties ~~over multiple stations~~ over the TP and the aerosol  
10 properties and sources during the high aerosol ~~pollution events~~ loading in over the TP ~~based on~~  
11 ~~multiple years of five ground-based sunphotometer observations and the MODIS aerosol optical~~  
12 ~~depth product in TP.~~ In addition, we ~~will~~ also combined the observation and models to study the  
13 aerosol transport process over the TP, thereby helping to reduce the uncertainties in estimate  
14 estimating of aerosol radiative forcing and aerosol sources.

15  
16 In this paper, section 2 describes the observation sites, data and methods ~~are~~. The results of the  
17 analysis of the spatiotemporal-spatial variations ~~of in~~ aerosol properties over the TP ~~is are~~ shown in  
18 ~~Section section~~ 3. The analysis of aerosol ~~pollution high loading~~ and an aerosol transport case are  
19 presented in section 4 and 5, respectively. The conclusions are presented in section 6.

## 20 21 **2. Site, data and ~~Methodology~~ methodology**

### 22 **2.1 ~~site~~ Sites**

23 In this study, five sites in the TP equipped with ~~the~~ sun and sky scanning radiometers (CE318)  
24 were used (Figure 1). Table 1 shows the station locations and descriptions. Lhasa station is the only  
25 urban site ~~where that can~~ suffers from ~~the~~ local anthropogenic emissions. ~~As f~~ For the other four sites,  
26 local anthropogenic emissions are extremely rare due to ~~few signs~~ the low number of human  
27 ~~habitation inhabitants~~. However, Mt\_WLG is in the northeast of the TP, where it is situated ~~at on~~  
28 the dust transport path from the ~~maximal largest~~ desert ~~of in~~ China (the Taklimakan Desert). The  
29 Muztagh\_Ata site is located in the northwest corner of the TP and ~~beside next to~~ the Central Asian  
30 Desert ~~Areas~~ and the Taklimakan Desert. NAM\_CO is located ~~in on~~ the central Tibetan Plateau,  
31 220 km away from Lhasa. QOMS\_CAS is located at the northern slope of Mt. Qomolangma on the  
32 border of Tibet and Nepal. Therefore, these five sites ~~can stand for~~ are representative of the spatial  
33 features of the TP.

### 34 35 **2.2 Data**

#### 36 **2.2.1 CE318 aerosol optical properties**

37 The column-integrated aerosol properties over the five TP sites are derived from CE318  
38 measurements. Table 1 ~~has showed~~ shows the observation period. The CE318 instrument measures  
39 direct solar spectral radiation and the angular distribution of sky radiance. These spectral radiances  
40 can be used to ~~retrieval retrieve~~ aerosol optical parameters (such as aerosol optical depth (AOD))  
41 based on Beer's Law, ~~and~~ aerosol microphysical properties (such as volume size distribution) and  
42 ~~its the~~ radiative forcing ~~features~~ through radiation transfer theory (Dubovik and King, 2000;  
43 Dubovik et al., 2006). The instruments were periodically calibrated using the Langley method at  
44 AERONET global calibration sites (the Izaña, Spain or the Mauna Loa, USA) or using the inter-

1 comparison calibration method at the Beijing-CAMS site (Che et al., 2015). The cloud-screened and  
2 quality-controlled data of AOD, Extinction Ångstrom exponent (EAE), and aerosol volume size  
3 distribution ( $dV(r)/d\ln r$ ) are used in this work (Giles et al., 2019). Eck et al. (1999) showed that the  
4 uncertainty of the AOD was ~~about~~ approximately 0.01 to 0.02. The EAE is-was calculated from the  
5 AOD at 440 and 870 nm. The errors of retrieval for  $dV(r)/d\ln r$  ~~are-were~~ less than 10% in the maxima  
6 of the  $dV(r)/d\ln r$  and may increase up to 35% for the minimum values of  $dV(r)/d\ln r$  within the radius  
7 range between 0.1  $\mu\text{m}$  and 7  $\mu\text{m}$ ; for the edges of the retrieval size, the errors increased d apparently,  
8 ~~which doesbut did~~ not significantly affect the derivation of the main feature of  $dV(r)/d\ln r$  (Dubovik  
9 et al., 2002).

### 11 2.2.2 The MODIS AOD product

12 The Moderate Resolution Imaging Spectroradiometer (MODIS) instrument is a multi-spectral  
13 sensor with a wide spectral range from 0.4 to 14.4  $\mu\text{m}$  in 36 wavelength bands, onboard the Terra  
14 (morning descending direction~~s~~) and Aqua (afternoon ascending direction~~s~~) satellites in polar orbit,  
15 ~~respectively~~. It's broad swath of 2330 km permits retrieval aerosol products to cover the global word  
16 within 1-2 days. In this study, both Terra and Aqua MODIS Collection 6 Deep-Blue (DB) ~~and~~ Dark-  
17 Target (DT) combined AOD at 550 nm product with 10km spatial resolution (~~MODIS\_AOD~~) (Levy  
18 et al., 2013) from 2006 to 2017 ~~are-were~~ used. The MODIS AOD at 550 nm (MODIS\_AOD)  
19 combined the DT and DB algorithms merges the products from the two algorithms based on the  
20 normalized difference vegetation index (NDVI) statistics as follows: 1) the DT AOD data are used  
21 for NDVI > 0.3; 2) the DB AOD data are used for NDVI < 0.2; and 3) the mean of both the  
22 algorithms or AOD data with high quality flag are used for 0.2 ≤ NDVI ≤ 0.3. The MODIS\_AOD  
23 has been widely-validated in the global or regional areas (Bilal et al., 2018; Ma et al., 2016; Sayer  
24 et al., 2014). The root-mean-square error of MODIS\_AOD was about 0.13, and the percentage of  
25 MODIS\_AOD data within the expected error was larger-more than 71% at the Kunming site, which  
26 ~~around~~ is near the TP (Zhu et al., 2016).

### 28 2.2.3 The CALIOP profile data

29 The Cloud-Aerosol Lidar with Orthogonal Polarization (CALIOP), the primary instrument on  
30 board of CALIPSO satellite, is a near-nadir viewing two wavelength (532 nm and 1064 nm)  
31 polarization-sensitive lidar ~~which-that~~ performs global vertical profiles measurements of aerosols  
32 and clouds (Winker et al., 2010). It provides three primary calibrated and geolocated profile products  
33 ~~of profiles~~: total attenuated backscatter at 532 nm and 1064 nm and the perpendicular polarization  
34 component at 532 nm. The ~~data-CALIOP (version 4.10) products~~ used in this study include the  
35 attenuated backscattering coefficient profiles from ~~level~~ Level 1B and the vertical feature mask data  
36 products of aerosol subtype from level 2 products under 15 km altitude, which ~~are-were~~ downloaded  
37 from the Langley Atmospheric Science Data Center (ASDC). Kumar et al. (2018) have showed that  
38 the AOD from CALIOP version 4.10 agreed with the ground-based CE318 observation at a site in  
39 the central Himalayas with a correlation > 0.9 and ~ 87 % matchup data were within the expected  
40 error.

## 43 2.3 Methodology

44 The ground-based CE318 observations and MODIS AOD products ~~are-were analyzed~~ analysed

1 to show the spatiotemporal~~spatial~~ variations of~~in~~ aerosol properties in TP.

2  
3 The CE318 observed AOD at 440 nm with values larger than 0.4 at each site ~~is was considered~~  
4 as specially analysed to study the aerosol properties of the high aerosol ~~pollution-loading~~ over the  
5 TP. The value of 0.4 was selected because the mean annual values of AOD observed by CE318  
6 instruments at the TP sites were less than ~0.1 in the past studies (Xia et al., 2016; Cong et al., 2009),  
7 and this value is normally regarded as the high aerosol loading (Eck et al., 2010; Giles et al., 2012).  
8 ~~The b~~Back trajectories ~~are were~~ used for the aerosol source analysis in the TP. ~~The b~~Back trajectories  
9 ~~for on~~ the high aerosol ~~pollution-loading~~ study days ~~are were~~ calculated by using the Hybrid Single-  
10 Particle Lagrangian Integrated Trajectory (HYSPLIT) model which is driven by the one degree  
11 horizontal resolution archived meteorological fields with (Draxler and Hess, 1998). 72-hour back  
12 trajectories ending at the five sites at 10 m above ground level at 12 UTC on the days ~~of with high~~  
13 aerosol ~~pollution-loading~~ (AOD at 440 nm >0.4) ~~are were~~ used to identify the air mass sources.

14  
15 ~~A Case case study of long-range aerosol transport to the TP is was selected~~ based on the ground  
16 CE318 observations over Lhasa, NAM\_CO and QOMS\_CAS. ~~By combing The~~ HYSPLIT back  
17 trajectories, ~~and the~~ MODIS and CALIOP products were used to show the potential aerosol sources,  
18 spatial aerosol loading and the vertical features of the aerosol over the TP during the case period.  
19 In addition, ~~and~~ the Goddard Earth Observing System (GEOS)-Chem chemistry transport model,  
20 was used to simulate the AOD and its components (dust and carbon aerosol) during the case period,  
21 which may reflect the change in aerosol type during the case period.~~the aerosol source and type~~  
22 ~~during the case is analyzed.~~

23  
24 The GEOS-Chem chemical transport model (version 11-01) coupled with the online radiative  
25 transfer calculations (RRTMG) at  $0.5^\circ \times 0.667^\circ$  horizontal resolution over ~~the~~ East Asia domain  
26 (Bey et al., 2001; Wang et al., 2004) ~~is was~~ used ~~to simulate aerosol variation during the case period.~~  
27 The model was driving by the Global Modeling and Assimilation Office (GMAO) MERRA-2  
28 meteorology with the temporal resolution of 3 hours for meteorological parameters and 1 hour for  
29 surface fields. The simulation type of full chemistry in the troposphere was selected. The  
30 implementation of RRTMG in GEOS-Chem was described in Heald et al. (2014). The AOD was  
31 calculated according to Martin et al. (2003). The default global anthropogenic emissions were  
32 overwritten over East Asia by the MIX inventory from Li et al. (2014). The Global Fire Emission  
33 Database (GFED) (van der Werf et al., 2010) has been used to specify emissions from fire. The  
34 ~~default~~ More details on the configuration schemes respectively for advection, transport, convection,  
35 ~~deposition, model~~ and the other emissions data used and the evaluation of AOD in the east and south  
36 of the TP were shown in Zhu et al. (2017).

37 ~~are used for the model simulation of full chemistry.~~

38 In this study, the AOD from the CE318, MODIS, and GEOS-Chem model were used. For  
39 convenience, CE318 AOD, MODIS AOD, and Model AOD stand for the AOD observed by  
40 CE318, MODIS, and the AOD simulated by the GEOS-Chem model, respectively. For  
41 CE318 AOD, the 440 nm wavelength is often studied, while MODIS AOD and Model AOD  
42 generally use the data at 550 nm wavelength. Thus, unless otherwise specified, CE318 AOD,  
43 MODIS AOD, and Model AOD hereinafter represent the ones at 440 nm, 550 nm, and 550 nm,  
44 respectively.

### 3. Temporal-spatial variations of aerosol properties

#### 3.1 Temporal variation of aerosol properties observed by the CE318 instruments

The monthly, seasonal, and annual variations in aerosol properties observed from the CE318 instruments at the five TP sites were analyzed.

Annual variation of CE318 AOD and EAE over TP at the four sites, i.e. Lhasa, Mt\_WLG, NAM\_CO, and QOMS\_CAS are shown in Figure 2. The data of the CE318 observation at Muztagh\_Ata site are available only during 2010, thus the annual variation at this site is not shown here. The annual AOD shows increased trends of  $0.001 \pm 0.003/\text{year}$  at Lhasa,  $0.013 \pm 0.003/\text{year}$  at Mt\_WLG, and  $0.002 \pm 0.002/\text{year}$  at NAM\_CO during CE318 observed period. Mt\_WLG site shows the most obvious increase of AOD during 2009–2013. These indicate the increase of aerosol loading in the three sites. The long term annual variation of AOD at QOMS\_CAS is very small ( $0.000 \pm 0.002/\text{year}$ ), but there still exists short term annual variation (decreased from 2010 to 2013 and increased from 2013 to 2016). The annual trends of EAES show more evident than the AOD in these four sites. Most sites show the increased tendency of annual averaged EAE, except for Mt\_WLG sites with a large decreasing trend of  $-0.318 \pm 0.081/\text{year}$ . This showed the size of aerosol at Mt\_WLG sites increased, while the size of aerosol decreased in other three sites. Combining the AOD and EAE, the positive trend of AOD with the positive trend of EAE in the long term at most sites over TP indicates the addition of fine mode aerosol mainly from the anthropogenic impact. But in the short term, the increase of annual averaged AOD is often with the decrease of EAE over TP, which suggests the addition of coarse mode aerosol during the CE318 observation.

The monthly and seasonal statistics variations of CE318 AOD and EAE at the five sites over the TP are shown in Figure 3 and Table 2, respectively. Distinct monthly and seasonal variability of the AOD and EAE over the five sites can be found. The monthly mean CE318 AOD shows the highest value in April at the Lhasa (0.19), NAM\_CO (0.09) and QOMS\_CAS (0.10) sites, while the value at Mt\_WLG was highest in June (0.20). The monthly mean CE318 AOD rapidly increases from January to April, and then slightly decreases until December at the Lhasa, NAM\_CO and QOMS\_CAS sites. However, the monthly mean CE318 AOD at Mt\_WLG shows almost symmetry is nearly symmetrical form from January to December. The monthly variation of EAE is different from the AOD at each site. The highest monthly EAE values occurs in September at Lhasa (1.15), October at Mt\_WLG (1.15) and in January at the NAM\_CO (0.93) and QOMS\_CAS (0.17) sites. The EAE at QOMS\_CAS also shows a high value of 0.17 in April, which may be caused by the smoke aerosol transported from South Asia during this period. The monthly mean EAE first decreases firstly from January to March, and then increases until September at Lhasa. The monthly mean EAE values at NAM\_CO also decreases from January to March, but does not increase apparently in the following months. The EAE at Mt\_WLG decreases from January to May and then increases obviously from May to October. The Lhasa, NAM\_CO, and QOMS\_CAS sites are near and located in the south of the TP. Thus, the variations of aerosol properties at these three sites are similar. The Mt\_WLG site is located in the northeast of the TP, which is different from the southern sites. The Muztagh\_Alt is in the northwest of the TP and is the nearest closest site to the Taklimakan Desert, which causes the high AOD there (a few observed data may be another reason).

1 ~~Looking at~~ ~~Combining~~ the monthly CE318 AOD and EAE values together, ~~the~~ high  
2 CE318 AOD is often accompanied by ~~the~~ low EAE at Lhasa, Mt\_WLG and NAM\_CO,  
3 indicating that these sites suffered from ~~the~~ coarse aerosols such as dust (Huang et al., 2007; Liu et  
4 al., 2015; Zhang et al., 2001). However, the QOMS\_CAS sites show ~~the~~ high CE318 AOD  
5 and high EAE at-in April, which ~~is~~ may be related to ~~the~~ smoke aerosols transported from South  
6 Asia.

7  
8 Table 2 shows the seasonal statistics of CE318 AOD and EAE. A distinct seasonal variation  
9 in CE318 AOD and EAE ~~variation~~ can be found over the TP sites. The CE318 AOD  
10 mean values in fall (SON) and winter (DJF) are lower at all sites except Muztagh. Muztagh\_Ata  
11 shows high CE318 AOD in both observed seasons. Except for that in Muztagh, the ~~maximal~~  
12 maximum seasonal CE318 AOD is observed in spring (MAM) (Lhasa, NAM\_CO, and  
13 QOMS\_CAS) or in summer (JJA) (Mt\_WLG). The ~~minimal~~ minimum seasonal EAE occurred in  
14 spring (Lhasa, NAM\_CO and Mt\_WLG) or summer (QOMS\_CAS), while the maximal ~~maximum~~  
15 EAE values is-are mostly observed in fall (Lhasa and Mt\_WLG) and winter (NAM\_CO and  
16 QOMS\_CAS). These indicate frequently dust events over the TP in the spring period at Lhasa,  
17 NAM\_CO and Mt\_WLG. Mt\_WLG is situated at-on the dust transport path from the Taklimakan  
18 Desert, which causes the high CE318 AOD observed in spring and summer ~~in-at~~ this site.

19  
20 The seasonal size distributions of the five sites in ~~Figure 3~~ Figure 4 also demonstrate that coarse  
21 mode aerosol is dominant at the five TP sites in almost all seasons, which is different from those in  
22 the eastern pollution regions of China ~~with fine mode aerosol dominant~~, such as Yangtze River Delta,  
23 where fine mode aerosol is dominant (Zhuang et al., 2018). ~~These~~ This size distribution explained  
24 the relatively lower annual averages of EAE ~~in-at~~ the five sites (all annual ~~-EAE in Figure 2 are~~  
25 less than <1.0), ~~which was lower than~~ compared to the those at the inland urban and suburban sites  
26 in China (Xin et al., 2007), ~~for the example of such as~~ Beijing (1.19) (Fan et al., 2006), Nanjing  
27 (1.20) (Zhuang et al., 2018; Zhuang et al., 2017), Kunming (1.25) (Zhu et al., 2016), and Chengdu  
28 (1.09) (Che et al., 2015). What's more, spring is the season with a high-high volume concentration  
29 of coarse mode aerosol. Among the five sites, the southernmost sites, QOMS\_CAS, showed the  
30 highest mean EAE and the size distribution was distinctly bimodal, especially in spring. This was  
31 also because of the frequently biomass burning activity in India and Nepal, which can transport the  
32 fine aerosol to the QOMS\_CAS site.

33  
34 The annual averages of CE318 AOD (shown in Figure 2) are 0.05-0.14 over TP sites. These  
35 average values are lower than those in other regional background sites, such as Longfengshan (0.35)  
36 in Northeast China (Wang et al., 2010), Xinglong (0.28) in North China Plain (Zhu et al., 2014),  
37 Lin'an (0.89) in Eastern China (Pan et al., 2010) and Dinghushan (0.91) in Southern China (Chen  
38 et al., 2014). The low aerosol loading over the five TP sites indicates excellent air quality over the  
39 TP region.

40  
41 However, the aerosol loading at the TP sites presents interannual changes. The annual  
42 variations in CE318 AOD and EAE over TP at the four sites, i.e. Lhasa, Mt\_WLG, NAM\_CO, and  
43 QOMS\_CAS are shown in Figure 4. The data for the CE318 observations at Muztagh\_Ata site are  
44 only available for 2010; thus, the annual variation at this site is not shown here. The annual

1 CE318 AOD shows increasing trends of  $0.001 \pm 0.003/\text{year}$  at Lhasa,  $0.013 \pm 0.003/\text{year}$  at  
2 Mt. WLG, and  $0.002 \pm 0.002/\text{year}$  at NAM. CO during the CE318 observation period. The Mt. WLG  
3 site shows the most obvious increase in CE318 AOD during 2009-2013. These results indicate an  
4 increase in aerosol loading at the three sites. The long-term annual variation of CE318 AOD at  
5 QOMS CAS is very small ( $0.000 \pm 0.002/\text{year}$ ), but there are still short-term annual variations (the  
6 values decreased from 2010 to 2013 and increased from 2013 to 2016). The annual trends of EAEs  
7 are more evident than the CE318 AOD at these four sites. Most sites show an increasing tendency  
8 in the average annual EAE except for Mt. WLG site, which shows a large decreasing trend of  $-0.318$   
9  $\pm 0.081/\text{year}$ . This shows that the size of aerosol at the Mt. WLG site increased, while the size of the  
10 aerosol decreased in the other three sites. Looking at the CE318 AOD and EAE values together,  
11 the positive trend of CE318 AOD and the positive trend of EAE in the long term variation at most  
12 sites over TP indicates the addition of fine mode aerosol which may be related to the anthropogenic  
13 impact or long-distance transport of dust to the TP. However, in the short term, the increase in the  
14 average annual CE318 AOD is often associated with the decrease in EAE over the TP, which  
15 suggests the addition of coarse mode aerosol during the CE318 observation period.

### 16 17 **3.2 Spatial variation of aerosol properties from MODIS**

18 Ground-based observations can offer accurate aerosol optical properties at point locations but  
19 lack spatial coverage. The MODIS aerosol product can provide the spatial variation in AOD over  
20 the TP. Thus, we evaluated the MODIS AOD using the ground-based observation CE318 AOD at  
21 550 nm over the TP sites. The CE318 AOD at 550 nm was interpolated from 440 nm, 675 nm, 870  
22 nm and 1020 nm by using an established fitting method from Ångström (1929). The matchup  
23 method was that the CE318 data within 1 hour of the MODIS overpass were compared with the  
24 MODIS data within a 25 km radius of the ground-based site. The minimum requirement for a  
25 matchup was at least 3 pixels from MODIS.

26  
27 Figure 5 shows the results of MODIS AOD compared to the collocated ground CE318  
28 observations over the TP. There are 996 instantaneous matchups of Terra and Aqua MODIS during  
29 the CE318 instrument measurement period at the five TP sites. The MODIS AOD overestimates  
30 the AOD at 550 nm with a positive mean bias of 0.02 and a root mean squared error (RMSE) of  
31 0.11. The RMSE value is lower than that of the North China Plain sites ( $\sim 0.25$ ) (Bilal et al., 2019).  
32 The slope and intercept of the best-fit equation between the MODIS AOD and CE318 AOD at 550  
33 nm are 0.46 and 0.06, respectively, with a correlation coefficient (R) of 0.54. There are 67.8% of  
34 the compared AODs within the expected error envelope of  $0.05 + 0.15\text{AOD}$  (%EE). The R value is  
35 lower than that in the global assessment statistics, while the %EE is higher than that in the global  
36 evaluation (Bilal and Qiu, 2018). Overall, the results suggest that the MODIS AOD product can be  
37 used to study the aerosol spatial variation over the TP region.

38  
39 The spatial distribution of MODIS the annual MODIS AOD is shown in Figure 6  
40 5. The MODIS AOD agrees with the CE318 AOD at 550 nm  
41 observed by CE318 at the five TP sites. The northwest area around the Taklimakan Desert  
42 and the northern part of the TP on the transport path of the Taklimakan Desert dust showed  
43 the high MODIS AOD ( $>0.25$ ) in past-recent decades. In addition, besides, the southern edge  
44 performed slightly high MODIS AOD ( $0.2-0.25$ ) influenced by the aerosol transport from

1 South Asia. There ~~exists is~~ some ~~little-small~~ area with high ~~MODIS\_AOD~~AOD (~0.2) in the ~~center~~  
2 ~~centre~~ of ~~the~~ TP, and the southeast region ~~is shown of~~shows low ~~MODIS\_AOD~~AOD (~0.1), which  
3 may be attributed to the aerosol transport and surface features such as ~~vegetable-vegetation~~ cover,  
4 since there are few inhabitants. The seasonal departure of ~~MODIS-MODIS~~ AOD (Figure 7Figure  
5 6) shows that high positive ~~MODIS\_AOD~~AOD departure often appears in spring, especially for the  
6 northwest edge, north~~ern~~ area and south~~ern~~ edge of TP, which was a result ~~from-of~~the aerosol  
7 transport from the frequent dust events ~~at-in~~ the Taklimakan ~~Desert~~ and ~~the~~ fire activities in South  
8 Asia in spring.

9  
10 A linear regression ~~trend~~ analysis of ~~the trends in~~ ~~MODIS-annual~~ ~~MODIS\_AOD~~AOD at 550nm  
11 over ~~the~~ TP from 2006 to 2017 was conducted using the least squares method. The spatial  
12 distribution of ~~the~~ annual trends in ~~MODIS-MODIS~~ AOD during 2006-2017 is illustrated in Figure  
13 ~~8Figure-7~~. There are no statistically significant trends in most areas during 2006-2007. The  
14 ~~MODIS\_AOD~~AOD ~~performed-showed~~ negative trends in the northwest edge close~~d~~ to ~~the~~  
15 Taklimakan Desert and ~~to~~ the east of the Qaidam Basin and slightly positive trends in most of the  
16 other areas. The ~~areas where MODIS\_AOD~~ ~~descending-decreased~~ ~~area-is~~ ~~are~~ mainly ~~located~~  
17 ~~the-place~~ near the desert or ~~lied-in-on~~ the transport path of ~~the~~ desert dust. This descending trend may  
18 be related to the significant reduction in dust emissions caused by the decline in wind speed in recent  
19 years (Yang et al., 2017b). The positive trend in other most areas may be due to the rapid increase  
20 in human activities, such as the ~~expend~~expansion of tourism to ~~the~~ TP and ~~the~~ biomass burning in  
21 South Asia.

22  
23 The seasonal trends ~~of-in~~ ~~MODIS-MODIS~~ AOD at 550 nm over ~~the~~ TP during 2006-2017 ~~is~~  
24 ~~are~~ presented in Figure 9Figure-8. The spring showed the most obvious ~~of-the~~ decline in  
25 ~~MODIS\_AOD~~AOD (~ 0.02/year) ~~in-at~~ the north~~ern~~ edges and northeast part of ~~the~~ TP during 2006  
26 -2017, which also suggested ~~that~~ the reduction ~~of-in~~ dust impact from the Taklimakan Desert ~~as-like~~  
27 the trend ~~of-in~~ the annual ~~MODIS-MODIS~~ AOD (seen in Figure 8Figure-7). In summer, the positive  
28 trend ~~of-in~~ ~~MODIS\_AOD~~AOD over ~~the~~ TP was relatively apparent, and most higher sporadic  
29 positive values of ~0.01 occurred in ~~the~~ central and south~~ern~~ part of ~~the~~ TP. Summer is the tourist  
30 season ~~over-in~~ the TP and ~~the~~ tourism has developed in past decades, which may be one of the  
31 reasons ~~of-for~~ the higher positive trend in summer in ~~the~~ TP. The ~~apparent~~ positive trends in autumn  
32 and winter were relatively ~~less-lower~~ than ~~those in~~ summer, and ~~the~~ most positive trends were  
33 located at the northern TP. The reason ~~of-for~~ this phenomenon needs to be explored.

#### 34 35 **4. Aerosol properties and potential sources during high aerosol loading**~~Aerosol pollution at~~ 36 ~~Tibetan-plateau~~

37 The ~~annual~~ mean AOD in ~~the~~ TP is normally low ~~for its little trace of~~due to the few human  
38 ~~inhabitants~~tion and high altitude. However, some high ~~CE318~~ AODs ~~with-values~~ larger than 0.4,  
39 ~~which is normally regarded as high aerosol loading~~ (Eck et al., 2010; Giles et al., 2012), ~~had~~  
40 ~~been~~were observed at the five sites in ~~the~~ TP by CE318. ~~Thus, the CE318\_AOD larger than 0.4 over~~  
41 ~~TP can be considered as the aerosol pollution. The frequencies of high aerosol loading~~  
42 ~~(CE318\_AOD > 0.4) during the CE318 measurements were 1.57%, 1.79%, 0.21%, 0.42% and 0.11%~~  
43 ~~at the Lhasa, Mt\_WLG, Muztagh\_Ata, NAM\_CO, and QOMS\_CAS sites, respectively.~~ The aerosol  
44 properties and sources ~~of-the-high-AOD (>0.4)~~during high aerosol loading in ~~the~~ TP need to be

1 studied.

2  
3 ~~Figure 10~~~~Figure 9~~ shows the ~~CE318\_AOD~~~~AOD~~ with values larger than 0.4 versus EAE  
4 observed by CE318 at the five sites in ~~the~~ TP. Except ~~for~~ the Lhasa and Mt\_WLG sites, almost all  
5 values of ~~CE318\_AOD~~~~AOD~~ are less than 1.0, which reflects the relatively clear environment over  
6 ~~the~~ TP. The EAE shows two ~~centers-centres~~ ~~of at~~ ~0.1 and ~1.5. The low EAE (~0.1) ~~center-centre~~  
7 is related to ~~the~~ dust events, which can cause higher concentrations of coarse particles in the  
8 atmosphere. Besides, most values of ~~the~~ low EAE (<0.5) part are less than 0.2 (only ~~a few of~~ EAEs  
9 between 0.2-0.5 ~~is-are~~ observed at Lhasa and Mt\_WLG), indicating ~~that~~ the pure dust type is more  
10 ~~common~~ than the polluted dust type in ~~the~~ TP according to Eck et al. (2010). The high EAE ~~center-~~  
11 ~~centre~~ ~~in-at~~ ~1.5 indicates ~~the~~ mainly small sub-micron radius particles, which ~~is-can be~~ attributed  
12 to ~~the~~ anthropologic emissions. ~~There-can-be found that~~ the values of EAE >1.0 ~~part-at~~ ~~the~~ NAM\_CO  
13 and QOMS\_CAS ~~sites~~ are generally higher than ~~those at the~~ Lhasa and Mt\_WLG sites. According  
14 to ~~the~~ past studies, the EAE of biomass burning aerosol is generally ~~higher~~ than the urban/industry  
15 aerosol (Giles et al., 2012; Eck et al., 2010), which may cause the higher EAE at NAM\_CO and  
16 QOMS\_CAS (more biomass burning aerosol) than ~~at~~ Lhasa and Mt\_WLG (more urban/industry  
17 aerosol). On the other hand, the values ~~with-in~~ the middle ~~range~~ of 0.5-1.0 ~~is-are~~ rare, indicating the  
18 less mix of ~~nature-natural~~ and human sources. The percentage of EAE bins to the number of ~~CE318~~  
19 ~~CE318\_AOD~~>0.4 is distinct ~~from each other sites~~ (Table 3). The percentage of EAE <0.5 is high  
20 than that ~~of~~ EAE>1.0 at Lhasa, Mt\_WLG and Muztagh\_Atata, indicating more nature dust pollution  
21 than the ~~anthropologic-anthropogenic~~ pollution at these three sites. However, ~~more-a greater number~~  
22 ~~of~~ high EAE ~~values~~ (>1.0) ~~is-are~~ observed than EAE<0.5 at ~~the~~ NAM\_CO and QOMS\_CAS sites,  
23 suggesting that ~~anthropogenic-anthropologic~~ pollution is more than ~~nature-natural~~ dust pollution at  
24 these two sites.

25  
26 ~~Figure 11~~~~Figure 10~~ shows the aerosol size distribution binned by ~~CE318\_AOD~~~~AOD~~ at the five  
27 sites in ~~the~~ TP. The volume concentration of coarse mode particles increases more apparently than  
28 fine mode at Lhasa, Mt\_WLG and Muztagh sites when the values of ~~CE318\_AOD~~~~AOD~~ increase.  
29 However, the size distribution at NAM\_CO and QOMS\_CAS shows the dominant ~~increasing~~  
30 ~~increase~~ of fine mode aerosol. These indicate of the different aerosol type pollution in these five  
31 sites: dust dominant in Lhasa, Mt\_WLG and Muztagh and fine mode aerosol (mainly biomass  
32 burning aerosol) pollution dominant at NAM\_CO and QOMS\_CAS.

33  
34 The dominant aerosol pollution type showed ~~the-obvious distinctions~~ ~~in-among~~ the five sites ~~at~~  
35 ~~on the~~ TP, then where is the distinct aerosol pollution source at each site? We used ~~the~~ HYSPLIT  
36 back-trajectory model and ~~the MODIS-MODIS\_AOD~~ on the ~~day with~~ aerosol pollution ~~day~~ (~~CE318~~  
37 ~~CE318\_AOD~~ >0.4) to show the aerosol source on ~~the~~ pollution day at each site. ~~Figure 12~~~~Figure 11~~  
38 ~~is-shows~~ the 72 hour back-trajectories ended at the five site (10 m above ground level) in ~~the~~ TP  
39 overlaid ~~by-with~~ the mean ~~MODIS-MODIS\_AOD-at-550-nm~~ on the aerosol pollution day observed  
40 by ~~the~~ ground-based CE318 (~~CE318-CE318\_AOD~~ >0.4). The CE318 instruments ~~have~~ observed 78,  
41 20, 2, 15, ~~and~~ 14 days with instantaneous AOD at 440 nm > 0.4 at Lhasa, Mt\_WLG, Muztagh\_Atata,  
42 NAM\_CO and QOMS\_CAS, respectively. The aerosol pollution days at Lhasa, Mt\_WLG, and  
43 Muztagh\_Atata observed by CE318 are often with low EAE (black trajectories). The airflows ended  
44 ~~at~~ the Lhasa site on ~~the~~ polluted days are mainly from ~~the~~ northwest and southwest. The ~~MODIS~~

1 MODIS AOD around Lhasa in the area of the back-trajectories with CE318 EAE <0.5 passing does  
2 not show significantly high values, especially in the Taklimakan Desert, which indicates that the  
3 dust pollution at Lhasa is mainly from local or around-surrounding dust events rather than transport  
4 from the Taklimakan Desert. The Mt\_WLG shows that the air mass on the pollution days comes  
5 from the west and east and the way-path of back trajectories is-with has high MODIS-MODIS AOD.  
6 The high values of MODIS-MODIS AOD has-shown shows two transport paths of dust aerosol to  
7 Mt\_WLG: one is through the Qaidam Basin and another-the other is through the northeast edge of  
8 the TP. The two polluted days observed by CE318 at the Muztagh\_Ata shows the easterly airflows  
9 originated-originating from the Taklimakan Desert. The direction of the back-trajectories of  
10 EAE<0.5 that ended at NAM\_CO is similar to Lhasa, while the southerly air flows with high EAE  
11 (red trajectories) is originate~~d~~ from Nepal, where frequent biomass burning happened and caused  
12 the high MODIS-MODIS AOD values. The trajectories ended at QOMS\_CAS and the high MODIS  
13 MODIS AOD of its-passing the path has-shown revealed the the transport of smoke-finer aerosol  
14 from South Asia to this site.

## 15 16 **5. Case study of long-range transport to the TP**

17 The long-range transport of aerosol can cause the aerosol pollution and affect the long-term  
18 variation in aerosol over the TP. In addition, the dominant aerosol type may change at the TP sites  
19 during a case of aerosol transport. Thus, A a specific case of aerosol pollution during 27 April - 3  
20 May 2016 is-was analyzed-analysed further. This case is selected based on the observations of-from  
21 the CE318 instrument. During 28 April -1 May, the CE318 AOD AOD-observed-by-CE318 at Lhasa,  
22 NAM\_CO, QOMS\_CAS sites showed up the values larger than 0.4, which value reached up to more  
23 than 3 times of the mean values of CE318 AOD AOD of each site (0.11 at Lhasa, 0.05 at NAM\_CO  
24 and QOMS\_CAS). This is-was indicative of the aerosol pollution at the three sites. Then, how about  
25 the aerosol properties of this period and where did the polluted aerosol come from?

26  
27 Figure 13 Figure-12 shows the daily CE318 AOD AOD and EAE during 27 April – 03 May at  
28 the three sites. The mean values of CE318 AOD AOD-from-CE318-Sun-photometer were 0.45, 0.38,  
29 and 0.23 at Lhasa, NAM\_CO and QOMS\_CAS, respectively. These even reached to 4 times of the  
30 annual mean CE318 AOD AOD at each site. The mean EAEs were 0.98, 1.22, and 1.44 at Lhasa,  
31 NAM\_CO and QOMS\_CAS, respectively, which was relative higher than the annual averages and  
32 suggested the fine aerosol entrance. There were CE318 AOD AOD peaks at the three sites during  
33 27 April – 03 May. Lhasa showed the-an increase of CE318 AOD AOD from 0.30 on 27 April to  
34 0.51 on 28 April, and kept-maintained high CE318 AOD AOD to a value of 0.54 on 1 May, after  
35 that-which it decreased to 0.34 on 2 May. NAM\_CO also showed the-an increase of  
36 CE318 AOD AOD at-during the first two days of the period, but decreased after 29 April.  
37 QOMS\_CAM showed a slight increase of-in CE318 AOD AOD from 27 April to 40-30 April, which  
38 was later than those of the other two sites. Combining the EAE on these days, fine mode aerosol  
39 was brought in-to Lhasa and NAM\_CO during 27-29 April, and then coarse aerosol began to  
40 occurred on 30 April, and even became the dominant aerosol in the following several days. The fine  
41 aerosol at the QOMS\_CAM site kept-were maintained for an extra-additional day than-after those  
42 at the two sites, and then the coarse aerosol increased.

43  
44 The GEOS-Chem model simulation also supported the above results. Figure 14 Figure-13

1 shows the comparison between the ~~GEOS-Chem model simulated AOD~~ Model AOD ( $0.5^\circ \times 0.667^\circ$ )  
2 and ~~CE318-observed~~ CE318 AOD at 550 nm and the ratios of the model simulated aerosol types  
3 (dust, both organic carbon (OC) and black carbon (BC) aerosol) to the total ~~Model AOD~~ AOD  
4 during this case period at the three sites. The evaluation results showed that the model  
5 underestimated the daily AOD at the three sites during ~~the~~ this period, with negative mean biases  
6 from -0.28 to -0.08. However, the ~~Model AOD~~ model AOD was relatively high correlated with the  
7 ~~CE318~~ CE318 AOD at 550 nm, with the correlation coefficient (R) values of 0.61 at Lhasa, 0.89 at  
8 NAM\_CO and 0.86 at QOMS\_CAS. These R values were higher than the model evaluation in South  
9 China and the Indo-China Plain (~0.5) (Zhu et al., 2017). Thus, ~~AOD~~ the variation trend from  
10 ~~Model AOD~~ the model simulation was in good agreement agreed well with that measured by the  
11 CE318 instruments during these days. During the first 4 days of the case period (27 April to 30  
12 April), the ratios of different aerosols to ~~the~~ total Model AOD ~~AOD~~ showed that the sum of OC and  
13 BC aerosols was ~~were~~ higher than those of dust aerosol at all ~~the~~ three sites. Besides, the sums of  
14 OC and BC at Lhasa and QOMS\_CAS was ~~were~~ higher than that of NAM\_CO. These indicated  
15 that the smoke aerosol affected the three sites more severely than dust during the first 4 days and  
16 Lhasa and QOMS\_CAS sites were nearer to smoke sources than NAM\_CO. After 30 April, the sum  
17 of BC and OC was ~~decreased~~ while dust increased, and the increase of dust at the three sites was  
18 NAM\_CO > Lhasa > QOMS\_CAS. Therefore, the major aerosol source was changed and the  
19 NAM\_CO site was closer to dust source after ~~40-30~~ April. This phenomenon had continued to 2  
20 May at NAM\_CO and Lhasa, and 1 May at QOMS\_CAS. ~~At~~ In the last one or two days, the dust  
21 decreased while the smoke obviously ~~obviously~~ increased, which could cause the mixture of ~~this~~  
22 these two aerosols.

23  
24 Then, how ~~is~~ was the spatial aerosol loading around the TP and the vertical feature of aerosol  
25 transported to the TP? ~~Figure 15~~ Figure 14 shows ~~MODIS-C6~~ the MODIS AOD at 550nm and 72-  
26 hour ~~h~~ back trajectories at Lhasa (the first row), the CALIOP-derived vertical profile of total  
27 attenuated backscatter at 532 nm (the second row), and the vertical feature mask of aerosol (the third  
28 row) on 28 April ~~28~~, 1 May ~~1~~, and 3 May ~~3~~ during ~~this~~ the case study period. The ~~MODIS~~  
29 MODIS AOD showed high values in the south (South Asia) and north (Taklimakan Desert) on the  
30 three days. The ~~H~~ high values in South Asia was ~~were~~ caused by anthropogenic aerosols (such as  
31 biomass burning) or dust polluted by anthropogenic aerosols, while the high MODIS AOD in the  
32 Taklimakan Desert was ~~resulted from~~ the dust. The values and areas of the high MODIS AOD in  
33 South Asia and Taklimakan Desert on 1 May ~~1~~ and 3 May ~~3~~ were higher and larger than ~~that~~ those  
34 on April 28. The back-~~trajectories~~ trajectories ended at Lhasa on the three days were different. On 28 April,  
35 the air flows were ~~originated~~ from the southwest (South Asia region). However, the air masses on 1  
36 and 3 May were from the northwest (Taklimakan Desert).

37  
38 The CALIPSO ground tracks across the TP and through South Asia and the Taklimakan Desert  
39 were chosen to show the aerosol transport to the TP sites. On 28 April, the ~~level~~ Level-1 attenuated  
40 backscatter at 532 nm derived from CALIOP (the second row) showed apparent aerosol layers in  
41 the ~~S~~ southern area (Bhutan and northeast India) and this aerosol layer even lifted ~~extended~~ to an  
42 altitude of ~10km ~~altitude in the sky~~ over the TP along the southern slope of the TP. On 1 May, the  
43 CALIOP attenuated backscatter not only showed the deep aerosol layers in south of the TP but also  
44 showed stronger aerosol layers ~~in the~~ in the north of the TP (Taklimakan Desert area). Besides, the north

1 aerosol layers also climbed into the air over the TP, but not as high as the southern aerosol layer. On  
2 3 May, there were also aerosol layers ~~on~~ in the south and north of the TP and ~~they that both~~ were  
3 both transported to above the TP ~~overhead~~, but the aerosol loading over the TP was lower than that  
4 on 28 April and 1 May (the values of attenuated backscatter on 3 May was lower), which ~~caused~~  
5 corresponds to the lower CE318 AOD ~~observed by CE318 at the three TP sites (Figure 12)~~ on this  
6 day ~~was lower than those on~~ 28 April and 1 May at the three TP sites (Figure 13).

7  
8 The vertical feature mask of the aerosol from CALIOP (the third row) ~~shows~~ showed the  
9 aerosol types on the three days. On 28 April, the aerosol layer in the north (~~about ~~~ 35°N) and above  
10 the TP was mainly the smoke aerosol and was even higher than 10 km. The back trajectories ended  
11 at Lhasa also showed that the southern airflow brought the smoke aerosol and polluted dust from  
12 South Asia to the ~~center~~ centre of the TP. On 1 May, the aerosol layer ~~in~~ on the southern slope of the  
13 TP was also ~~the~~ smoke aerosol and polluted dust, while the aerosol layers in the northern ~~of~~ TP and  
14 above the TP ~~overhead~~ were almost all dust aerosol, which could be explained by the northwest  
15 airflows carrying the dust aerosol from the Taklimakan Desert. which ~~These~~ may be the result of  
16 the lower EAE values at Lhasa and NAM\_CO than that at QOMS\_CAM (~~Figure 13~~ Figure 12). ~~After~~  
17 ~~two days mixing, On 3 May,~~ the aerosol type above the central TP and the southern TP ~~on 3 May~~  
18 ~~has been~~ was occupied by ~~the~~ polluted dust aerosol, and the EAE at NAM\_CO and QOMS\_CAM  
19 also showed a little slight increase on 3 May. These results agree with the aerosol simulation ~~of from~~  
20 GEOS-Chem. Jia et al. (2015) has shown that the dust from India polluted by anthropogenic aerosols  
21 can be transported to the TP, but the back trajectories on 1 and 3 May illustrated that the airflows  
22 that ended at Lhasa were from the north or northwest rather than the south, indicating that the  
23 polluted dust over the TP on 3 May was more likely the mixing result of dust and smoke aerosol. In  
24 addition, the lengths of the back trajectories (especially the back trajectories at 10 m and 500 m  
25 above ground level) on 1 May showed that the airflows moved slowly, which allowed the possibility  
26 of aerosol mixture over the TP. The observations and model simulations illustrated a the following  
27 scene: ~~firstly,~~ the smoke aerosol in South Asia was lifted up to 10 km, ~~eontaminated~~ contaminating  
28 the TP sites, and transported to the centre of the TP; then, the dust from the Taklimakan Desert  
29 could climb the north slope of the TP and be transported to the TP; finally, the dust and smoke  
30 aerosol over the TP were mixed ~~at last~~. This case of aerosol pollution shows that the anthropogenic  
31 aerosols (mainly smoke) smoke in South Asia and Dust dust in the Taklimakan Desert could be  
32 transported to the center centre of the TP and they both even can cause ~~the~~ mixed aerosol pollution  
33 above the TP. The past cases ~~studies~~ of aerosol transport to the TP are almost individual dust or  
34 smoke aerosol, while this case of aerosol pollution over the TP ~~has shown~~ showed the mixing  
35 pollution during the last two days of the case period.

## 36 37 6. Conclusion

38 The long-term ~~temporal spatial~~ spatiotemporal variations ~~of in the~~ aerosol optical properties  
39 and the impacts of the aerosol long-range aerosol transport ~~impact~~ over the TP were ~~analyzed~~  
40 analysed by using a combination of ground-based and satellite remote sensing aerosol products as  
41 well as model simulations. The major conclusions are drawn as follows:

- 42 (1) The annual CE318 AOD at most TP sites showed increasing trends (0–0.013/year) during the  
43 past decade: 0.001±0.003/year at Lhasa, 0.013±0.003/year at Mt\_WLG, 0.002±0.002/year at  
44 NAM\_CO, and 0.000±0.002/year at QOMS\_CAS. ~~Most sites showed the i~~ Increaseding

1 ~~tendency tendencies of in the~~ annual-averaged EAE, ~~except for Mt\_WLG~~ were also found at  
2 ~~most TP~~ sites ~~with a large decreasing trend of 0.318/year~~. Spatially, the MODIS AOD showed  
3 negative trends in the northwest edge closed to the Taklimakan Desert and the east of Qaidam  
4 Basin and slightly positive trends in most of the other areas of the TP.

5 (2) ~~The values of EAE with AOD>0.4 at five TP ground stations showed two centers of ~0.1 and~~  
6 ~~-1.5. The EAE and size distribution during the aerosol polluted day (CE318 AOD at 440 nm >~~  
7 ~~0.4) at the TP showed the different aerosol type pollution in the five sites: dust dominant in~~  
8 ~~Lhasa, Mt\_WLG and Muztagh and fine mode aerosol pollution dominant at NAM\_CO and~~  
9 ~~QOMS\_CAS. The back trajectories on polluted days indicated the dust aerosol mainly come~~  
10 ~~from the Taklimakan Desert and fine mode aerosol was mainly transported from South~~  
11 ~~Asia.~~ Different aerosol types and sources contributed to the high aerosol loading at the five sites:  
12 dust was dominant in Lhasa, Mt\_WLG and Muztagh with sources from the Taklimakan Desert,  
13 but fine aerosol pollution was dominant at NAM\_CO and QOMS\_CAS with the transport from  
14 South Asia.

15 (3) A case of smoke followed by dust pollution at Lhasa, NAM\_CO and QOMS\_CAS during 28  
16 April – 3 May 2016 ~~was analyzed: showed that~~ ~~–firstly,~~ the smoke aerosol in South Asia was  
17 first uplifted up to 10 km and transported to the center centre of TP; ~~then~~ Then, the dust from  
18 the Taklimakan Desert could climb the northern slope of the TP and be transported to the TP,  
19 allowing the dust and smoke aerosol over the TP were to mixed at last.

20  
21 There are some limitations in this study. First, ground-based remote sensing and MODIS  
22 MODIS AOD products may have had missing data due to missed conditions interfered with clouds  
23 interference. Second, only half of a year of observations at the Muztagh\_Ata station may not be  
24 sufficient to fully reveal pollution days in the northwest TP region, which will could have affected  
25 the statistics to some extent. More long-term in situ observations are needed in the TP. However,  
26 due to the remoteness and challenging weather conditions over the plateau, maintaining long-term  
27 in situ observation stations over the TP ~~in long term~~ is very difficult. The numerical model  
28 simulation is more practically feasible to study the aerosol properties over the TP, but the model  
29 accuracy is far from being ideal over the TP. Thus, long-term numerical model simulation coupling  
30 coupled with satellite observations and intensive short-term field campaigns should be used to  
31 analyze ~~analyse~~ the aerosol properties over the TP in the future.

#### 32 33 Data availability:

34 The four sites (Mt\_WLG, Muztagh\_Ata, NAM\_CO and QOMS\_CAS) data are available from  
35 AERONET website (<https://aeronet.gsfc.nasa.gov/>). The dataset of Lhasa used in the study can be  
36 requested by contacting the corresponding author. The MODIS aerosol products are available from  
37 <http://ladsweb.nascom.nasa.gov>. The HYSPLIT model and meteorological fields' data can be from  
38 <https://www.arl.noaa.gov/hysplit/>. The CALIPSO data are from <https://eosweb.larc.nasa.gov>.  
39 GEOS-Chem model code and share data can be obtained from [http://wiki.seas.harvard.edu/geos-](http://wiki.seas.harvard.edu/geos-chem)  
40 chem.

#### 41 42 Competing interests.

43 The authors declare that they have no conflict of interest.  
44

1 Author contribution:

2 All authors help to shape the ideas and review this manuscript. JZ, XX and HC designed, and  
3 wrote the manuscript; JZ, XX, HC, JW help to analyze the data; HC, XZ, SK and ZC carried out  
4 the sunphotometer observations; JW, ZC, SK, TZ, XY, and YZ provided constructive comments on  
5 this study.

6

7 **Acknowledgments**

8 This research was supported by the National Science Fund for Distinguished Young Scholars  
9 (41825011), the National Key R & D Program Pilot Projects of China (2016YFA0601901 and  
10 2016YFC0203304), the National Natural Science Foundation of China (41761144056), the  
11 Strategic Priority Research Program of Chinese Academy of Sciences (XDA20040500), the Natural  
12 Science Foundation of Jiangsu Province (BK20170943), the Open fund by the Key Laboratory for  
13 Middle Atmosphere and Global Environment Observation (LAGEO) / Institute of Atmospheric  
14 Physics, and LAC/CMA (2018B02).

15

## References

- Ångström, A.: On the atmospheric transmission of Sun radiation and on dust in the air, *Geografiska Annaler*, 11, 156-166, <https://doi.org/10.1080/20014422.1929.11880498>, 1929.
- Bey, I., Jacob, D. J., Yantosca, R. M., Logan, J. A., Field, B. D., Fiore, A. M., Li, Q., Liu, H. Y., Mickley, L. J., and Schultz, M. G.: Global modeling of tropospheric chemistry with assimilated meteorology: Model description and evaluation, *Journal of Geophysical Research: Atmospheres*, 106, 23073-23095, <https://doi.org/10.1029/2001jd000807>, 2001.
- Bilal, M., Nazeer, M., Qiu, Z., Ding, X., and Wei, J.: Global Validation of MODIS C6 and C6.1 Merged Aerosol Products over Diverse Vegetated Surfaces, *Remote Sens-Basel*, 10, 475, <https://doi.org/10.3390/rs10030475>, 2018.
- Bilal, M., and Qiu, Z.: Evaluation of Modis C6 Combined Aerosol Product at Global Scale, *IGARSS 2018 - 2018 IEEE International Geoscience and Remote Sensing Symposium*, 2018, 9126-9129.
- Bilal, M., Nazeer, M., Nichol, J., Qiu, Z., Wang, L., Bleiweiss, M. P., Shen, X., Campbell, J. R., and Lolli, S.: Evaluation of Terra-MODIS C6 and C6.1 Aerosol Products against Beijing, XiangHe, and Xinglong AERONET Sites in China during 2004-2014, *Remote Sens-Basel*, 11, 486, <https://doi.org/doi:10.3390/rs11050486>, 2019.
- Che, H., Zhang, X. Y., Xia, X., Goloub, P., Holben, B., Zhao, H., Wang, Y., Zhang, X. C., Wang, H., Blarel, L., Damiri, B., Zhang, R., Deng, X., Ma, Y., Wang, T., Geng, F., Qi, B., Zhu, J., Yu, J., Chen, Q., and Shi, G.: Ground-based aerosol climatology of China: aerosol optical depths from the China Aerosol Remote Sensing Network (CARSNET) 2002–2013, *Atmospheric Chemistry and Physics*, 15, 7619-7652, <https://doi.org/10.5194/acp-15-7619-2015>, 2015.
- Che, H. Z., Wang, Y. Q., and Sun, J. Y.: Aerosol optical properties at Mt. Waliguan Observatory, China, *Atmospheric Environment*, 45, 6004-6009, <https://doi.org/10.1016/j.atmosenv.2011.07.050>, 2011.
- Chen, J., Xin, J., An, J., Wang, Y., Liu, Z., Chao, N., and Meng, Z.: Observation of aerosol optical properties and particulate pollution at background station in the Pearl River Delta region, *Atmospheric Research*, 143, 216-227, <https://doi.org/10.1016/j.atmosres.2014.02.011>, 2014.
- Cong, Z., Kang, S., Liu, X., and Wang, G.: Elemental composition of aerosol in the Nam Co region, Tibetan Plateau, during summer monsoon season, *Atmospheric Environment*, 41, 1180-1187, <https://doi.org/10.1016/j.atmosenv.2006.09.046>, 2007.
- Cong, Z., Kang, S., Smirnov, A., and Holben, B.: Aerosol optical properties at Nam Co, a remote site in central Tibetan Plateau, *Atmospheric Research*, 92, 42-48, <https://doi.org/10.1016/j.atmosres.2008.08.005>, 2009.
- Draxler, R. R., and Hess, G. D.: An overview of the HYSPLIT-4 Modelling system for trajectories, dispersion and deposition, *Australian Meteorological Magazine*, 47, 295-308, 1998.
- Du, W., Sun, Y. L., Xu, Y. S., Jiang, Q., Wang, Q. Q., Yang, W., Wang, F., Bai, Z. P., Zhao, X. D., and Yang, Y. C.: Chemical characterization of submicron aerosol and particle growth events at a national background site (3295 m a.s.l.) on the Tibetan Plateau, *Atmospheric Chemistry and Physics*, 15, 10811-10824, <https://doi.org/10.5194/acp-15-10811-2015>, 2015.
- Dubovik, O., and King, M. D.: A flexible inversion algorithm for retrieval of aerosol optical properties from Sun and sky radiance measurements, *Journal of Geophysical Research: Atmospheres*, 105, 20673-20696, <https://doi.org/10.1029/2000jd900282>, 2000.
- Dubovik, O., Holben, B., Eck, T. F., Smirnov, A., Kaufman, Y. J., King, M. D., Tanré, D., and

1 Slutsker, I.: Variability of Absorption and Optical Properties of Key Aerosol Types Observed  
2 in Worldwide Locations, *Journal of the Atmospheric Sciences*, 59, 590-608,  
3 [https://doi.org/10.1175/1520-0469\(2002\)059<0590:voaaop>2.0.co;2](https://doi.org/10.1175/1520-0469(2002)059<0590:voaaop>2.0.co;2), 2002.

4 Dubovik, O., Sinyuk, A., Lapyonok, T., Holben, B. N., Mishchenko, M., Yang, P., Eck, T. F., Volten,  
5 H., Munoz, O., Veihelmann, B., van der Zande, W. J., Leon, J. F., Sorokin, M., and Slutsker, I.:  
6 Application of spheroid models to account for aerosol particle nonsphericity in remote sensing  
7 of desert dust, *J Geophys Res-Atmos*, 111, D11208.11201-D11208.11234,  
8 <https://doi.org/10.1029/2005jd006619>, 2006.

9 Eck, T. F., Holben, B. N., Reid, J. S., Dubovik, O., Smirnov, A., O'Neill, N. T., Slutsker, I., and  
10 Kinne, S.: wavelength dependence of the optical depth of biomass burning, urban, and desert  
11 dust aerosols, *Journal of Geophysical Research*, 104, 31,333-331,349,  
12 <https://doi.org/10.1029/1999JD900923>, 1999.

13 Eck, T. F., Holben, B. N., Sinyuk, A., Pinker, R. T., Goloub, P., Chen, H., Chatenet, B., Li, Z., Singh,  
14 R. P., Tripathi, S. N., Reid, J. S., Giles, D. M., Dubovik, O., O'Neill, N. T., Smirnov, A., Wang,  
15 P., and Xia, X.: Climatological aspects of the optical properties of fine/coarse mode aerosol  
16 mixtures, *J Geophys Res-Atmos*, 115, <https://doi.org/10.1029/2010jd014002>, 2010.

17 Fan, X., Chen, H., Goloub, P., Xia, X., Zhang, W., and Chatenet, B.: Analysis of column-integrated  
18 aerosol optical thickness in Beijing from AERONET observations, *China Particuology*, 4, 330-  
19 335, [https://doi.org/10.1016/S1672-2515\(07\)60285-1](https://doi.org/10.1016/S1672-2515(07)60285-1), 2006.

20 Giles, D. M., Holben, B. N., Eck, T. F., Sinyuk, A., Smirnov, A., Slutsker, I., Dickerson, R. R.,  
21 Thompson, A. M., and Schafer, J. S.: An analysis of AERONET aerosol absorption properties  
22 and classifications representative of aerosol source regions, *J Geophys Res-Atmos*, 117, 127-  
23 135, <https://doi.org/10.1029/2012JD018127>, 2012.

24 Giles, D. M., Sinyuk, A., Sorokin, M. G., Schafer, J. S., Smirnov, A., Slutsker, I., Eck, T. F., Holben,  
25 B. N., Lewis, J. R., Campbell, J. R., Welton, E. J., Korokin, S. V., and Lyapustin, A. I.:  
26 Advancements in the Aerosol Robotic Network (AERONET) Version 3 database – automated  
27 near-real-time quality control algorithm with improved cloud screening for Sun photometer  
28 aerosol optical depth (AOD) measurements, *Atmos Meas Tech*, 12, 169-209,  
29 <https://doi.org/10.5194/amt-12-169-2019>, 2019.

30 Heald, C. L., Ridley, D. A., Kroll, J. H., Barrett, S. R. H., Cady-Pereira, K. E., Alvarado, M. J., and  
31 Holmes, C. D.: Contrasting the direct radiative effect and direct radiative forcing of aerosols,  
32 *Atmospheric Chemistry and Physics*, 14, 5513-5527, [https://doi.org/10.5194/acp-14-5513-](https://doi.org/10.5194/acp-14-5513-2014)  
33 [2014](https://doi.org/10.5194/acp-14-5513-2014), 2014.

34 Huang, J., Minnis, P., Yi, Y., Tang, Q., Wang, X., Hu, Y., Liu, Z., Ayers, K., Trepte, C., and Winker,  
35 D.: Summer dust aerosols detected from CALIPSO over the Tibetan Plateau, *Geophys Res Lett*,  
36 34, 529-538, <https://doi.org/10.1029/2007gl029938>, 2007.

37 Jia, R., Liu, Y., Chen, B., Zhang, Z., and Huang, J.: Source and transportation of summer dust over  
38 the Tibetan Plateau, *Atmospheric Environment*, 123, 210-219,  
39 <https://doi.org/10.1016/j.atmosenv.2015.10.038>, 2015.

40 Kopacz, M., Mauzerall, D., Wang, J., Leibensperger, E., Henze, D., and Singh, K.: Origin and  
41 radiative forcing of black carbon transported to the Himalayas and Tibetan Plateau,  
42 *Atmospheric Chemistry and Physics*, 11, 2837-2852, [https://doi.org/10.5194/acp-11-2837-](https://doi.org/10.5194/acp-11-2837-2011)  
43 [2011](https://doi.org/10.5194/acp-11-2837-2011), 2011.

44 Kumar, A., Singh, N., Anshumali, and Solanki, R.: Evaluation and utilization of MODIS and

- 1 [CALIPSO aerosol retrievals over a complex terrain in Himalaya, Remote Sensing of](#)  
2 [Environment, 206, 139-155, <https://doi.org/10.1016/j.rse.2017.12.019>, 2018.](#)
- 3 Lau, K. M., Kim, M. K., and Kim, K. M.: Asian summer monsoon anomalies induced by aerosol  
4 direct forcing: the role of the Tibetan Plateau, *Clim Dynam*, 26, 855-864,  
5 <https://doi.org/10.1007/s00382-006-0114-z>, 2006.
- 6 Lee, W.-S., Bhawar, R. L., Kim, M.-K., and Sang, J.: Study of aerosol effect on accelerated snow  
7 melting over the Tibetan Plateau during boreal spring, *Atmospheric Environment*, 75, 113-122,  
8 <https://doi.org/10.1016/j.atmosenv.2013.04.004>, 2013.
- 9 Levy, R. C., Mattoo, S., Munchak, L. A., Remer, L. A., Sayer, A. M., Patadia, F., and Hsu, N. C.:  
10 The Collection 6 MODIS aerosol products over land and ocean, *Atmos Meas Tech*, 6, 2989-  
11 3034, <https://doi.org/10.5194/amt-6-2989-2013>, 2013.
- 12 Li, J., Huang, J., Stamnes, K., Wang, T., Lv, Q., and Jin, H.: A global survey of cloud overlap based  
13 on CALIPSO and CloudSat measurements, *Atmospheric Chemistry and Physics*, 15, 519-536,  
14 <https://doi.org/10.5194/acp-15-519-2015>, 2015.
- 15 Li, J., Lv, Q., Zhang, M., Wang, T., Kawamoto, K., Chen, S., and Zhang, B.: Effects of atmospheric  
16 dynamics and aerosols on the fraction of supercooled water clouds, *Atmospheric Chemistry*  
17 *and Physics*, 17, 1847-1863, <https://doi.org/10.5194/acp-17-1847-2017>, 2017.
- 18 Li, J., Jian, B., Huang, J., Hu, Y., Zhao, C., Kawamoto, K., Liao, S., and Wu, M.: Long-term  
19 variation of cloud droplet number concentrations from space-based Lidar, *Remote Sensing of*  
20 *Environment*, 213, 144-161, <https://doi.org/10.1016/j.rse.2018.05.011>, 2018.
- 21 Li, M., Zhang, Q., Streets, D. G., He, K. B., Cheng, Y. F., Emmons, L. K., Huo, H., Kang, S. C., Lu,  
22 Z., Shao, M., Su, H., Yu, X., and Zhang, Y.: Mapping Asian anthropogenic emissions of non-  
23 methane volatile organic compounds to multiple chemical mechanisms, *Atmospheric*  
24 *Chemistry and Physics*, 14, 5617-5638, <https://doi.org/10.5194/acp-14-5617-2014>, 2014.
- 25 Liu, Y., Sato, Y., Jia, R., Xie, Y., Huang, J., and Nakajima, T.: Modeling study on the transport of  
26 summer dust and anthropogenic aerosols over the Tibetan Plateau, *Atmospheric Chemistry and*  
27 *Physics*, 15, 12581-12594, <https://doi.org/10.5194/acp-15-12581-2015>, 2015.
- 28 Liu, Z., Liu, D., Huang, J., Vaughan, M., Uno, I., Sugimoto, N., Kittaka, C., Trepte, C., Wang, Z.,  
29 Hostetler, C., and Winker, D.: Airborne dust distributions over the Tibetan Plateau and  
30 surrounding areas derived from the first year of CALIPSO lidar observations, *Atmospheric*  
31 *Chemistry and Physics*, 8, 5045-5060, <https://doi.org/10.5194/acp-8-5045-2008>, 2008.
- 32 Lu, Z., Streets, D. G., Zhang, Q., and Wang, S.: A novel back-trajectory analysis of the origin of  
33 black carbon transported to the Himalayas and Tibetan Plateau during 1996-2010, *Geophys*  
34 *Res Lett*, 39, n/a-n/a, <https://doi.org/10.1029/2011gl049903>, 2012.
- 35 Ma, Y., Li, Z., Li, Z., Xie, Y., Fu, Q., Li, D., Zhang, Y., Xu, H., and Li, K.: Validation of MODIS  
36 Aerosol Optical Depth Retrieval over Mountains in Central China Based on a Sun-Sky  
37 Radiometer Site of SONET, *Remote Sens-Basel*, 8, 111, <https://doi.org/10.3390/rs8020111>,  
38 2016.
- 39 Martin, R. V., Jacob, D. J., Yantosca, R. M., Chin, M., and Ginoux, P.: Global and regional decreases  
40 in tropospheric oxidants from photochemical effects of aerosols, *J Geophys Res-Atmos*, 108,  
41 <https://doi.org/10.1029/2002jd002622>, 2003.
- 42 [Pan, L., Che, H., Geng, F., Xia, X., Wang, Y., Zhu, C., Chen, M., Gao, W., and Guo, J.: Aerosol](#)  
43 [optical properties based on ground measurements over the Chinese Yangtze Delta Region,](#)  
44 [Atmospheric Environment, 44, 2587-2596, <https://doi.org/10.1016/j.atmosenv.2010.04.013>,](#)

- 1        [2010](#).
- 2        Qian, Y., Flanner, M. G., Leung, L. R., and Wang, W.: Sensitivity studies on the impacts of Tibetan  
3        Plateau snowpack pollution on the Asian hydrological cycle and monsoon climate,  
4        *Atmospheric Chemistry and Physics*, 11, 1929-1948, [https://doi.org/10.5194/acp-11-1929-](https://doi.org/10.5194/acp-11-1929-2011)  
5        [2011](#), 2011.
- 6        Sayer, A. M., Munchak, L. A., Hsu, N. C., Levy, R. C., Bettenhausen, C., and Jeong, M. J.: MODIS  
7        Collection 6 aerosol products: Comparison between Aqua's e-Deep Blue, Dark Target, and  
8        “merged” data sets, and usage recommendations, *Journal of Geophysical Research:*  
9        *Atmospheres*, 119, 13,965-913,989, <https://doi.org/10.1002/2014jd022453>, 2014.
- 10       [Shen, R. Q., Ding, X., He, Q. F., Cong, Z. Y., Yu, Q. Q., and Wang, X. M.: Seasonal variation of](#)  
11       [secondary organic aerosol tracers in Central Tibetan Plateau, \*Atmospheric Chemistry and\*](#)  
12       [Physics, 15, 8781-8793, https://doi.org/10.5194/acp-15-8781-2015, 2015.](#)
- 13       Takemura, T., Nozawa, T., Emori, S., Nakajima, T. Y., and Nakajima, T.: Simulation of climate  
14       response to aerosol direct and indirect effects with aerosol transport-radiation model, *Journal*  
15       *of Geophysical Research*, 110, -, <https://doi.org/10.1029/2004jd005029>, 2005.
- 16       Tobo, Y., Iwasaka, Y., Shi, G.-Y., Kim, Y.-S., Ohashi, T., Tamura, K., and Zhang, D.: Balloon-borne  
17       observations of high aerosol concentrations near the summertime tropopause over the Tibetan  
18       Plateau, *Atmospheric Research*, 84, 233-241, <https://doi.org/10.1016/j.atmosres.2006.08.003>,  
19       2007.
- 20       [van der Werf, G. R., Randerson, J. T., Giglio, L., Collatz, G. J., Mu, M., Kasibhatla, P. S., Morton,](#)  
21       [D. C., DeFries, R. S., Jin, Y., and van Leeuwen, T. T.: Global fire emissions and the contribution](#)  
22       [of deforestation, savanna, forest, agricultural, and peat fires \(1997–2009\), \*Atmospheric\*](#)  
23       [Chemistry and Physics](#), 10, 11707-11735, <https://doi.org/10.5194/acp-10-11707-2010>, 2010.
- 24       Wan, X., Kang, S., Wang, Y., Xin, J., Liu, B., Guo, Y., Wen, T., Zhang, G., and Cong, Z.: Size  
25       distribution of carbonaceous aerosols at a high-altitude site on the central Tibetan Plateau (Nam  
26       Co Station, 4730ma.s.l.), *Atmospheric Research*, 153, 155-164,  
27       <https://doi.org/10.1016/j.atmosres.2014.08.008>, 2015.
- 28       [Wang, P., Che, H. Z., Zhang, X. C., Song, Q. L., Wang, Y. Q., Zhang, Z. H., Dai, X., and Yu, D. J.:](#)  
29       [Aerosol optical properties of regional background atmosphere in Northeast China,](#)  
30       [Atmospheric Environment](#), 44, 4404-4412, <https://doi.org/10.1016/j.atmosenv.2010.07.043>,  
31       [2010](#).
- 32       Wang, X., Ren, J., Gong, P., Wang, C., Xue, Y., Yao, T., and Lohmann, R.: Spatial distribution of  
33       the persistent organic pollutants across the Tibetan Plateau and its linkage with the climate  
34       systems: a 5-year air monitoring study, *Atmospheric Chemistry and Physics*, 16, 6901-6911,  
35       <https://doi.org/10.5194/acp-16-6901-2016>, 2016.
- 36       Wang, Y. X., McElroy, M. B., Jacob, D. J., and Yantosca, R. M.: A nested grid formulation for  
37       chemical transport over Asia: Applications to CO, *Journal of Geophysical Research:*  
38       *Atmospheres*, 109, n/a-n/a, <https://doi.org/10.1029/2004jd005237>, 2004.
- 39       Winker, D. M., Pelon, J., Coakley, J. A., Ackerman, S. A., Charlson, R. J., Colarco, P. R., Flamant,  
40       P., Fu, Q., Hoff, R. M., Kittaka, C., Kubar, T. L., Le Treut, H., McCormick, M. P., Megie, G.,  
41       Poole, L., Powell, K., Trepte, C., Vaughan, M. A., and Wielicki, B. A.: THE CALIPSO  
42       MISSION A Global 3D View of Aerosols and Clouds, *B Am Meteorol Soc*, 91, 1211-1229,  
43       <https://doi.org/10.1175/2010bams3009.1>, 2010.
- 44       Xia, X., Che, H., Zhu, J., Chen, H., Cong, Z., Deng, X., Fan, X., Fu, Y., Goloub, P., Jiang, H., Liu,

- 1 Q., Mai, B., Wang, P., Wu, Y., Zhang, J., Zhang, R., and Zhang, X.: Ground-based remote  
2 sensing of aerosol climatology in China: Aerosol optical properties, direct radiative effect and  
3 its parameterization, *Atmospheric Environment*, 124, 243-251,  
4 <https://doi.org/10.1016/j.atmosenv.2015.05.071>, 2016.
- 5 Xia, X. G., Wang, P. C., Wang, Y. S., Li, Z. Q., Xin, J. Y., Liu, J., and Chen, H. B.: Aerosol optical  
6 depth over the Tibetan Plateau and its relation to aerosols over the Taklimakan Desert, *Geophys  
7 Res Lett*, 35, 96-106, <https://doi.org/10.1029/2008gl034981>, 2008.
- 8 Xia, X. G., Zong, X. M., Cong, Z. Y., Chen, H. B., Kang, S. C., and Wang, P. C.: Baseline continental  
9 aerosol over the central Tibetan plateau and a case study of aerosol transport from South Asia,  
10 *Atmospheric Environment*, 45, 7370-7378, <https://doi.org/10.1016/j.atmosenv.2011.07.067>,  
11 2011.
- 12 Xin, J. Y., Wang, Y. S., Li, Z. Q., Wang, P. C., Hao, W. M., Nordgren, B. L., Wang, S. G., Liu, G. R.,  
13 Wang, L. L., Wen, T. X., Sun, Y., and Hu, B.: Aerosol optical depth (AOD) and Angstrom  
14 exponent of aerosols observed by the Chinese Sun Hazemeter Network from August 2004 to  
15 September 2005, *J Geophys Res-Atmos*, 112, 1703-1711,  
16 <https://doi.org/10.1029/2006jd007075>, 2007.
- 17 Xing, C., Liu, C., Wang, S., Chan, K. L., Gao, Y., Huang, X., Su, W., Zhang, C., Dong, Y., Fan, G.,  
18 Zhang, T., Chen, Z., Hu, Q., Su, H., Xie, Z., and Liu, J.: Observations of the vertical  
19 distributions of summertime atmospheric pollutants and the corresponding ozone  
20 production in Shanghai, China, *Atmospheric Chemistry and Physics*, 17, 14275-14289,  
21 <https://doi.org/10.5194/acp-17-14275-2017>, 2017.
- 22 Yang, R., Wang, J., Zhang, T., and He, S.: Change in the relationship between the Australian summer  
23 monsoon circulation and boreal summer precipitation over Central China in the late 1990s,  
24 *Meteorology and Atmospheric Physics*, 131, 105-113, [https://doi.org/10.1007/s00703-017-  
25 0556-3](https://doi.org/10.1007/s00703-017-0556-3), 2017a.
- 26 Yang, R. W., Tao, Y., and Cao, J.: A Mechanism for the Interannual Variation of the Early Summer  
27 East Asia-Pacific Teleconnection Wave Train, *Acta Meteorol Sin*, 24, 452-458, 2010.
- 28 Yang, Y., Russell, L. M., Lou, S., Liao, H., Guo, J., Liu, Y., Singh, B., and Ghan, S. J.: Dust-wind  
29 interactions can intensify aerosol pollution over eastern China, *Nature communications*, 8,  
30 15333, <https://doi.org/10.1038/ncomms15333>, 2017b.
- 31 Zhang, B., Wang, Y., and Hao, J.: Simulating aerosol–radiation–cloud feedbacks on meteorology  
32 and air quality over eastern China under severe haze conditions in winter, *Atmospheric  
33 Chemistry and Physics*, 15, 2387-2404, <https://doi.org/10.5194/acp-15-2387-2015>, 2015.
- 34 Zhang, N., Cao, J., Ho, K., and He, Y.: Chemical characterization of aerosol collected at Mt. Yulong  
35 in wintertime on the southeastern Tibetan Plateau, *Atmospheric Research*, 107, 76-85,  
36 <https://doi.org/10.1016/j.atmosres.2011.12.012>, 2012.
- 37 Zhang, X. Y., Arimoto, R., Cao, J. J., An, Z. S., and Wang, D.: Atmospheric dust aerosol over the  
38 Tibetan Plateau, *Journal of Geophysical Research: Atmospheres*, 106, 18471-18476,  
39 <https://doi.org/10.1029/2000jd900672>, 2001.
- 40 Zhao, Z., Cao, J., Shen, Z., Xu, B., Zhu, C., Chen, L. W. A., Su, X., Liu, S., Han, Y., Wang, G., and  
41 Ho, K.: Aerosol particles at a high-altitude site on the Southeast Tibetan Plateau, China:  
42 Implications for pollution transport from South Asia, *Journal of Geophysical Research:  
43 Atmospheres*, 118, 11,360-311,375, <https://doi.org/10.1002/jgrd.50599>, 2013.
- 44 Zhu, J., Che, H., Xia, X., Chen, H., Goloub, P., and Zhang, W.: Column-integrated aerosol optical

1 [and physical properties at a regional background atmosphere in North China Plain,](https://doi.org/10.1016/j.atmosenv.2013.11.019)  
2 [Atmospheric Environment, 84, 54-64, https://doi.org/10.1016/j.atmosenv.2013.11.019, 2014.](https://doi.org/10.1016/j.atmosenv.2013.11.019)

3 Zhu, J., Xia, X., Che, H., Wang, J., Zhang, J., and Duan, Y.: Study of aerosol optical properties at  
4 Kunming in southwest China and long-range transport of biomass burning aerosols from North  
5 Burma, Atmospheric Research, 169, 237-247, <https://doi.org/10.1016/j.atmosres.2015.10.012>,  
6 2016.

7 [Zhu, J., Xia, X., Wang, J., Zhang, J., Wiedinmyer, C., Fisher, J. A., and Keller, C. A.: Impact of](https://doi.org/10.1002/2016jd025793)  
8 [Southeast Asian smoke on aerosol properties in Southwest China: First comparison of model](https://doi.org/10.1002/2016jd025793)  
9 [simulations with satellite and ground observations, Journal of Geophysical Research:](https://doi.org/10.1002/2016jd025793)  
10 [Atmospheres, 122, 3904-3919, https://doi.org/10.1002/2016jd025793, 2017.](https://doi.org/10.1002/2016jd025793)

11 Zhuang, B. L., Wang, T. J., Liu, J., Li, S., Xie, M., Han, Y., Chen, P. L., Hu, Q. D., Yang, X. Q., Fu,  
12 C. B., and Zhu, J. L.: The surface aerosol optical properties in the urban area of Nanjing, west  
13 Yangtze River Delta, China, Atmospheric Chemistry and Physics, 17, 1143-1160,  
14 <https://doi.org/10.5194/acp-17-1143-2017>, 2017.

15 Zhuang, B. L., Wang, T. J., Liu, J. N. E., Che, H. Z., Han, Y., Fu, Y., Li, S., Xie, M., Li, M. M., Chen,  
16 P. L., Chen, H. M., Yang, X. Q., and Sun, J. N.: The optical properties, physical properties and  
17 direct radiative forcing of urban columnar aerosols in the Yangtze River Delta, China,  
18 Atmospheric Chemistry and Physics, 18, 1419-1436, [https://doi.org/10.5194/acp-18-1419-](https://doi.org/10.5194/acp-18-1419-2018)  
19 [2018](https://doi.org/10.5194/acp-18-1419-2018), 2018.

20  
21

1 **Figure captions**

2 Figure 1. Topography of the Tibetan Plateau (TP) and the five CE318 stations located in the TP  
3 (Lhasa, Mt\_WLG, Mutztagh\_Ata, NAM\_CO, and QOMS\_CAS).~~Figure 1. Topography of Tibetan~~  
4 ~~Plateau (TP) and the five CE318 stations located in TP (Lhasa, Mt\_WLG, Mutztagh\_Ata, NAM\_CO,~~  
5 ~~and QOMS\_CAS).~~

6 Figure 2. Box plots of the monthly AOD and EAE at the five sites located on the Tibetan Plateau,  
7 i.e., Lhasa, Mt\_WLG, Muztagh\_Alt, NAM\_CO, and QOMS\_CAS. In each box, the red-line in the  
8 centre is the median and the lower and upper limits are the first and the third quartiles, respectively.  
9 The lines extending vertically from the box indicate the spread of the distribution with the length  
10 being 1.5 times the difference between the first and the third quartiles. The asterisk symbols indicate  
11 the geometric means in each month. The annual mean values and standard errors are also shown in  
12 each subgraph.~~Figure 2. Box plots of monthly AOD and EAE at the five sites located in Tibetan~~  
13 ~~Plateau, i.e. Lhasa, Mt\_WLG, Muztagh\_Alt, NAM\_CO, and QOMS\_CAS. In each box, the central~~  
14 ~~red-line is the median and the lower and upper limits are the first and the third quartiles, respectively.~~  
15 ~~The lines extending vertically from the box indicate the spread of the distribution with the length~~  
16 ~~being 1.5 times the difference between the first and the third quartiles. The asterisk symbols indicate~~  
17 ~~the geometric means in each month. The annual mean values and standard errors are also shown in~~  
18 ~~each subgraph.~~

19 Figure 3. Seasonal variation in aerosol size distribution at the five sites located in Tibetan  
20 Plateau.~~Figure 3. Seasonal variation of aerosol size distribution at the five sites located in Tibetan~~  
21 ~~Plateau.~~

22 Figure 4. Annual averages of and trends in aerosol optical depth (AOD) and Extinction Ångstrom  
23 exponent (EAE) at four sites located in Tibetan Plateau.~~Figure 4. Annual average and the trends of~~  
24 ~~aerosol optical depth (AOD) and Extinction Ångstrom exponent (EAE) at four sites located in~~  
25 ~~Tibetan Plateau.~~

26 Figure 5. Comparisons of the 550 nm AOD measured by the CE318 instrument (CE318\_AOD) over  
27 Tibetan Plateau stations with the MODIS retrieval Deep-Blue/Dark-Target combined AOD of 10  
28 km spatial resolutions (MODIS\_AOD). The statistical parameters in this figure include the number  
29 of matchup data (N), the slope and intercept at the y-axis of linear regression (read line), the mean  
30 bias (MB), root mean squared error (RMSE), correlation coefficient (R), and the percentage of data  
31 within the expected error  $0.05+0.15AOD$  (%EE) which is used as the MODIS AOD expected  
32 uncertainty over land (green lines).~~Figure 5. Comparisons of AOD at 550nm measured by CE318~~  
33 ~~sunphotometer (CE318\_AOD) over Tibetan Plateau stations with the MODIS retrieval Deep-~~  
34 ~~Blue/Dark Target combined AOD of 10km spatial resolutions (MODIS\_AOD). The statistical~~  
35 ~~parameters in this figure include the number of matchup data (N), the slope and intercept at y axis~~  
36 ~~of linear regression (read line), the mean bias (MB), root mean squared error (RMSE), correlation~~  
37 ~~coefficient (R), and the percentage of data within the expected error  $0.05+0.15AOD$  (%EE) which~~  
38 ~~is used as the MODIS AOD expected uncertainty over land (green lines).~~

39 Figure 6. Spatial distribution of MODIS C6 AOD at 550 nm over the Tibetan Plateau (only the  
40 altitude > 3000 m) during 2006-2017. The color-filled circles are the CE318 observation AOD  
41 averages at TP sites.~~Figure 6. Spatial distribution of MODIS C6 AOD at 550nm over Tibetan Plateau~~

1 (only the altitude > 3000m) during 2006–2017. The circle with color filled is the CE318 observation  
2 AOD averages at TP sites.

3 Figure 7. The seasonal departure of MODIS AOD over the TP (altitude > 3000 m).~~Figure 7. The~~  
4 ~~seasonal departure of MODIS AOD over TP (altitude > 3000m).~~

5 Figure 8. Trend in the MODIS AOD at 550 nm during 2006–2017.~~Figure 8. Trend of MODIS AOD~~  
6 ~~at 550nm during 2006–2017.~~

7 Figure 9. Trends in the MODIS AOD at 550 nm during 2006–2017 in each season.~~Figure 9. Trends~~  
8 ~~of MODIS AOD at 550nm during 2006–2017 in each season.~~

9 Figure 10. AOD vs EAE (only CE318 AOD at 440 nm > 0.4 was considered) observed by CE318  
10 at the five sites on the Tibetan Plateau.~~Figure 10. AOD vs EAE (Only CE318 AOD at 440nm > 0.4~~  
11 ~~is considered) observed by CE318 at the five site Tibetan plateau.~~

12 Figure 11. Aerosol size distribution binned by CE318 AOD at the five sites on the Tibetan  
13 Plateau.~~Figure 11. Aerosol size distribution binned by CE318 AOD at the five sites in Tibetan~~  
14 ~~plateau.~~

15 Figure 12. The back-trajectories ended at the five sites (10 m above ground level) on the TP overlaid  
16 with the mean MODIS C6 AOD at 550 nm on the aerosol pollution day observed by ground-based  
17 CE318 (CE318 AOD > 0.4). Red stands for EAE > 1.0, black for EAE < 0.5, and green for EAE  
18 within 0.5–1.0.~~Figure 12. Back trajectories ended at the five site (10 m above ground level) in TP~~  
19 ~~overlaid by the mean MODIS C6 AOD at 550 nm on the aerosol pollution day observed by ground~~  
20 ~~base CE318 (CE318 AOD > 0.4). Red stands for EAE > 1.0, black is EAE < 0.5, and green is for EAE~~  
21 ~~within 0.5–1.0.~~

22 Figure 13. CE318 observed daily AOD at 440 nm and EAE during 27 April, 2016 – 3 May, 2016 at  
23 Lhasa, NAM\_CO and QOMS\_CAS.~~Figure 13. CE318 observed daily AOD at 440nm and EAE~~  
24 ~~during April 27, 2016 – May 3, 2016 at Lhasa, NAM\_CO and QOMS\_CAS.~~

25 Figure 14. The GEOS-Chem model simulated the daily average AOD vs CE318 observed daily  
26 AOD at 550 nm, and the ratios of dust or organic carbon (OC) and black carbon (BC) aerosol to the  
27 total AOD during 27 April, 2016 – 3 May, 2016 at Lhasa, NAM\_CO and QOMS\_CAS. The statistical  
28 parameters used in the modal evaluation are the same as those in Figure 5.~~Figure 14. The GEOS-~~  
29 ~~Chem model simulated daily average AOD vs CE318 observed daily AOD at 550nm, and the ratios~~  
30 ~~of dust or organic carbon (OC) and black carbon (BC) aerosol to the total AOD during April 27,~~  
31 ~~2016 – May 3, 2016 at Lhasa, NAM\_CO and QOMS\_CAS. The statistical parameters used in Modal~~  
32 ~~evaluation are same as Figure 5.~~

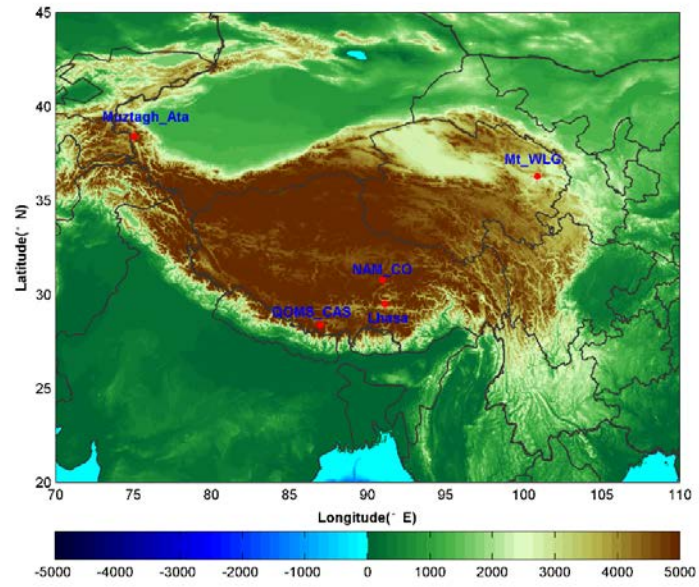
33 Figure 15. The MODIS C6 AOD at 550 nm and 72-hour back trajectories ended at Lhasa at three  
34 heights above the ground level (10 m in black, 500 m in red and 1000 m in blue lines) (the first row);  
35 the CALIOP-derived vertical profile of total attenuated backscatter at 532 nm (the second row); and  
36 the vertical feature mask of aerosol on 28 April, 1 May, and 3 May, 2016 over the ground track  
37 shown in the first row (green lines) (the third row).~~Figure 15. MODIS C6 AOD at 550 nm and 72h~~  
38 ~~back trajectories ended at Lhasa at three heights above the ground level (10 m with black, 500 m~~  
39 ~~with red and 1000 m with blue lines) (the first row), CALIOP-derived vertical profile of total~~

1 ~~attenuated backscatter at 532 nm (the second row), vertical feature mask of aerosol on April 28,~~  
2 ~~May 1, and May 3, 2016 over the ground track shown in the first row (green line) (the third row).~~

3

4

1



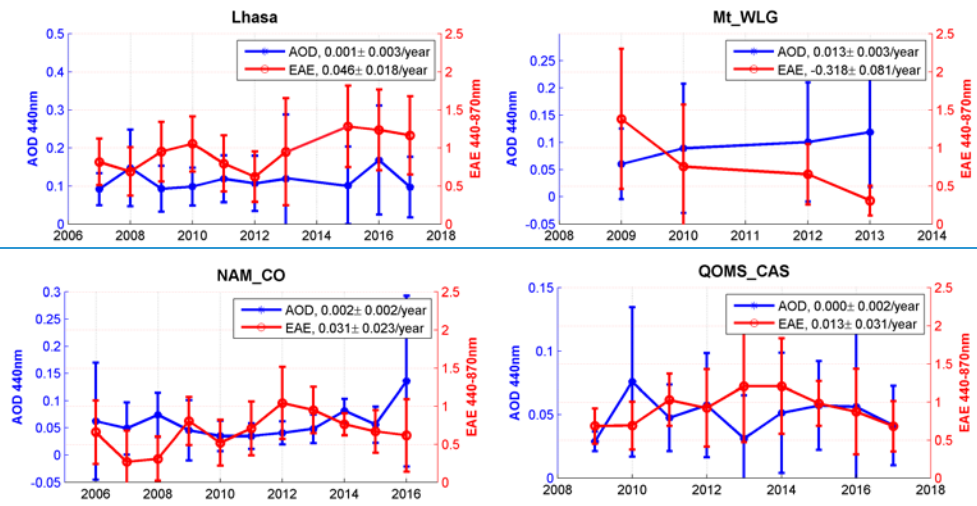
2

3

Figure 1. Topography of the Tibetan Plateau (TP) and the five CE318 stations located in the TP (Lhasa, Mt\_WLG, Mutztagh\_Ata, NAM\_CO, and QOMS\_CAS).

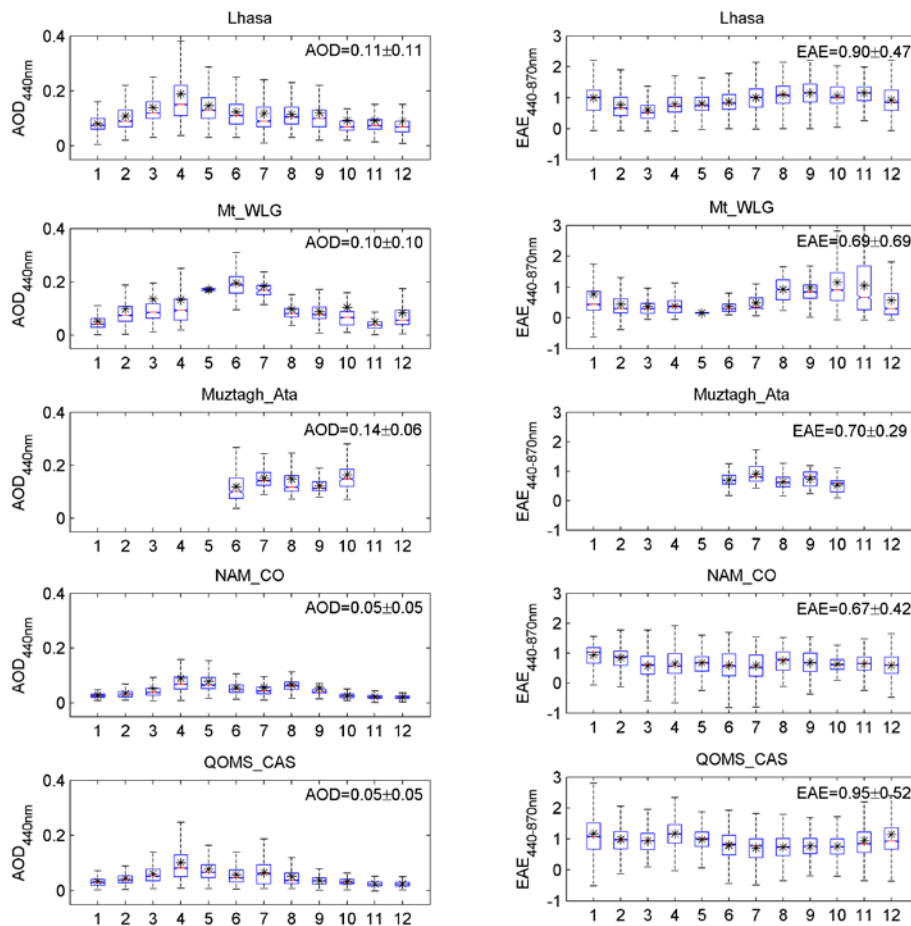
4

5



1  
2  
3  
4

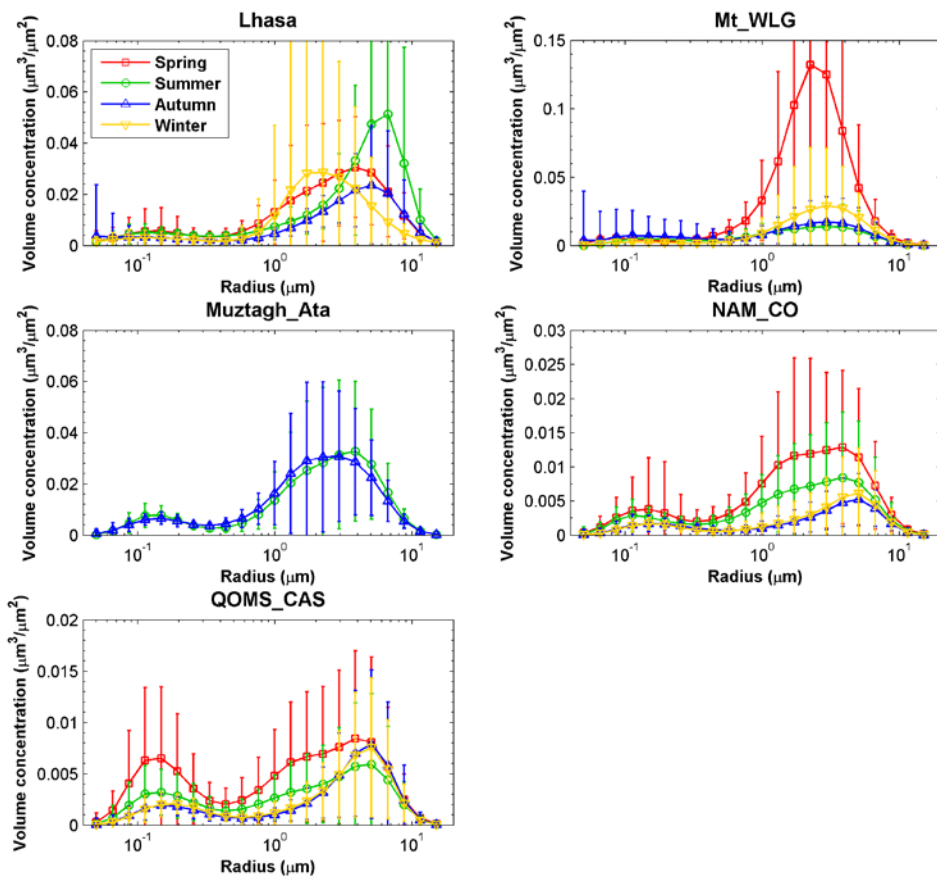
Figure 2. Annual average and the trends of aerosol optical depth (AOD) and Extinction Ångström exponent (EAE) at four sites located in Tibetan Plateau.



1

2 Figure 2. Box plots of the monthly AOD and EAE at the five sites located in on the Tibetan Plateau, i.e.,  
 3 Lhasa, Mt\_WLG, Muztagh\_Alt, NAM\_CO, and QOMS\_CAS. In each box, the central-red-line in the  
 4 centre is the median and the lower and upper limits are the first and the third quartiles, respectively. The  
 5 lines extending vertically from the box indicate the spread of the distribution with the length being 1.5  
 6 times the difference between the first and the third quartiles. The asterisk symbols indicate the geometric  
 7 means in each month. The annual mean values and standard errors are also shown in each subgraph.

8

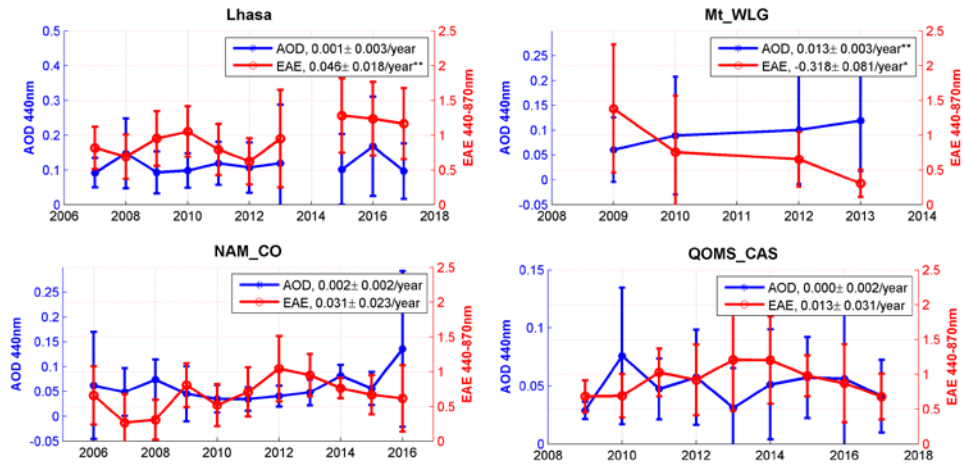


1

2 Figure 3. Seasonal variation of aerosol size distribution at the five sites located in Tibetan Plateau.

3

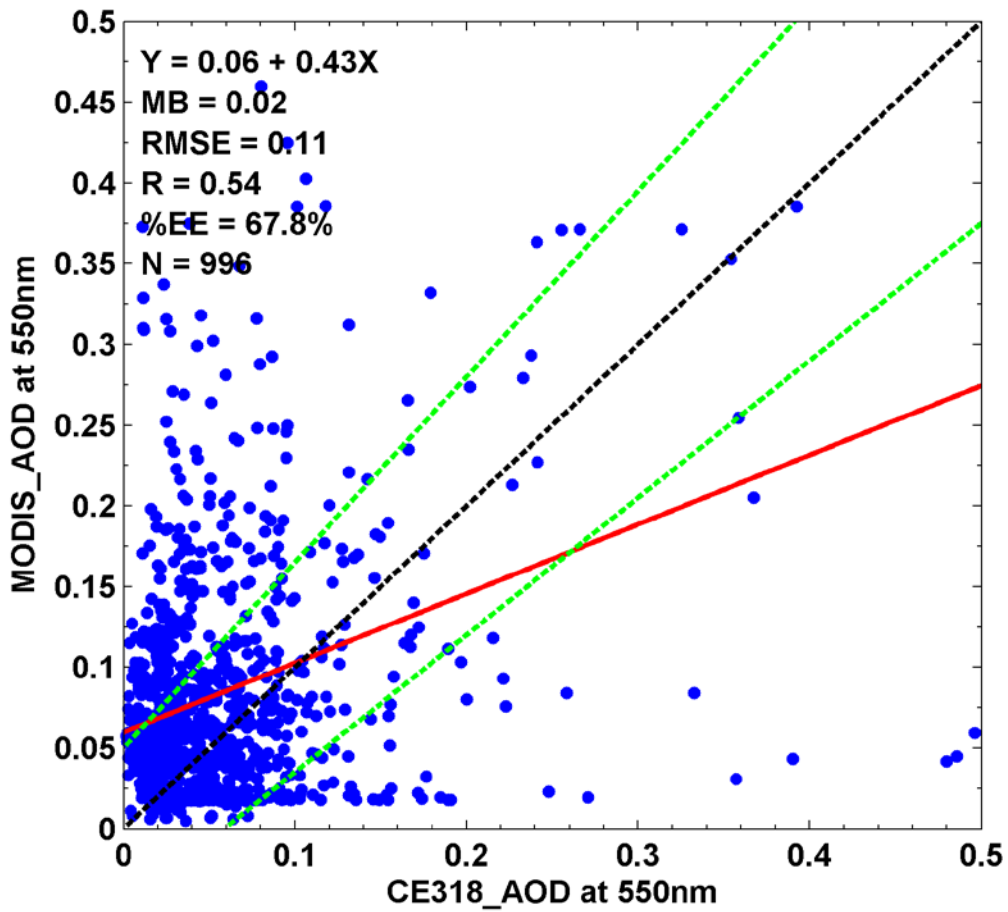
---



1  
2  
3  
4  
5

Figure 4. Annual averages of and trends in aerosol optical depth (AOD) and Extinction Ångstrom exponent (EAE) at four sites located in Tibetan Plateau. \* stands for 90% significance, and \*\* represents 95% significance.

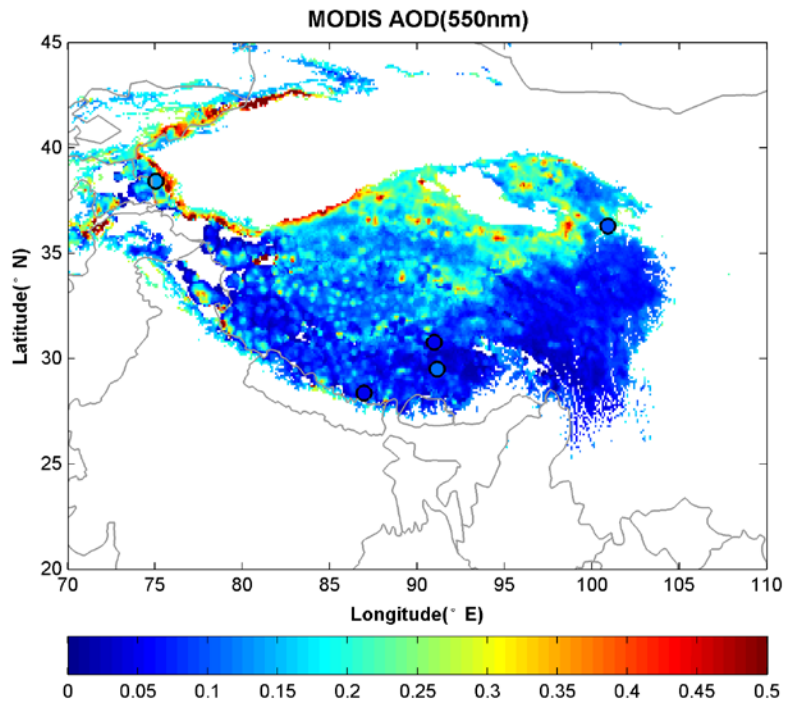
1



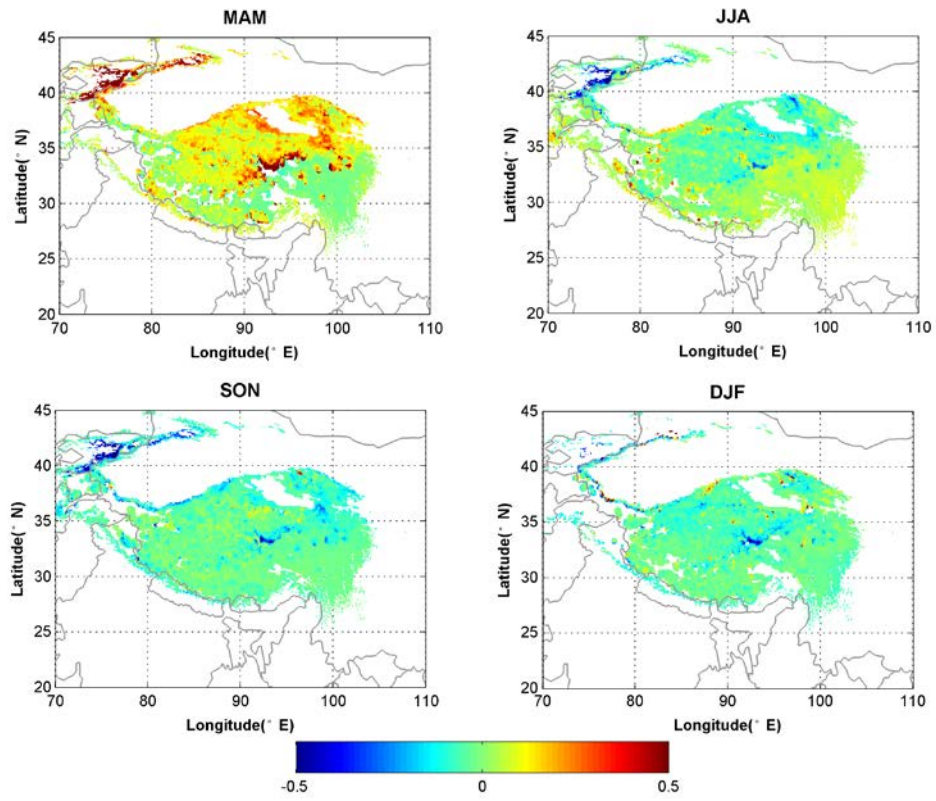
2

3 Figure 5. Comparisons of the 550 nm AOD measured by the CE318 instrument (CE318 AOD) over  
4 Tibetan Plateau stations with the MODIS retrieval Deep-Blue/Dark-Target combined AOD of 10 km  
5 spatial resolutions (MODIS AOD). The statistical parameters in this figure include the number of  
6 matchup data (N), the slope and intercept at the y-axis of linear regression (red line), the mean bias  
7 (MB), root mean squared error (RMSE), correlation coefficient (R), and the percentage of data within  
8 the expected error  $0.05+0.15AOD$  (%EE) which is used as the MODIS AOD expected uncertainty over  
9 land (green lines).

10

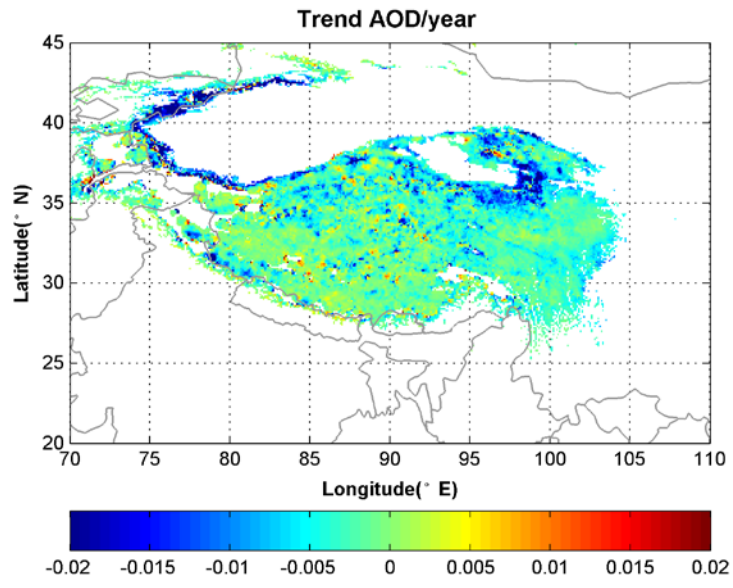


1  
 2 Figure 6. Spatial distribution of MODIS C6 AOD at 550\_nm over the Tibetan Plateau (only the altitude >  
 3 3000\_m) during 2006-2017. The color-filled circles with color filled is are the CE318 observation AOD  
 4 averages at TP sites.  
 5



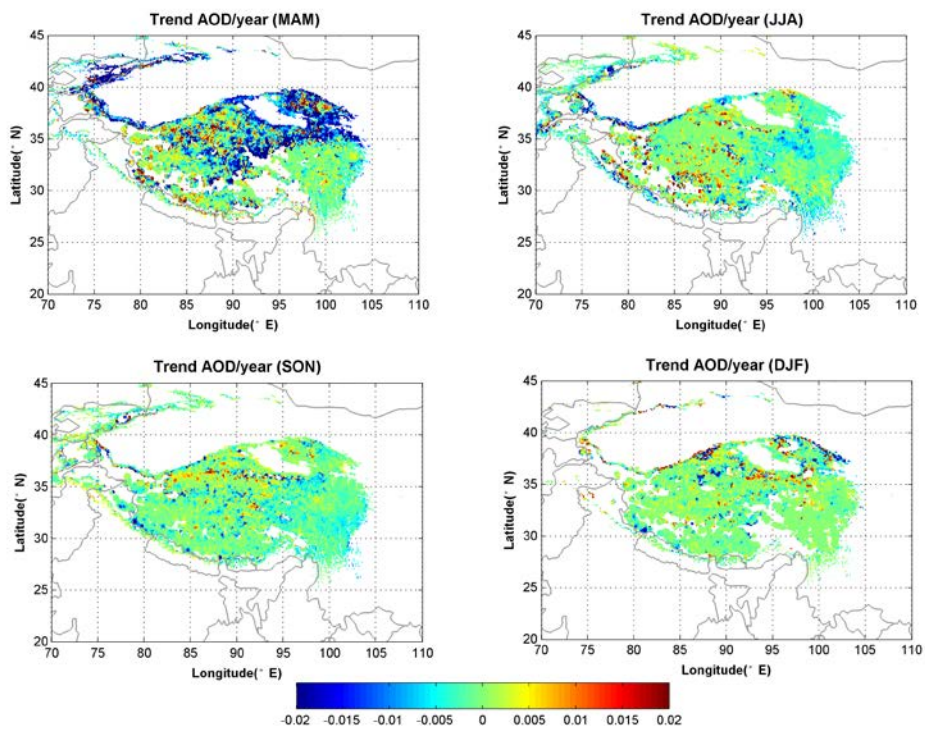
1  
2  
3

Figure 7. The seasonal departure of MODIS AOD over the TP (altitude > 3000 m).



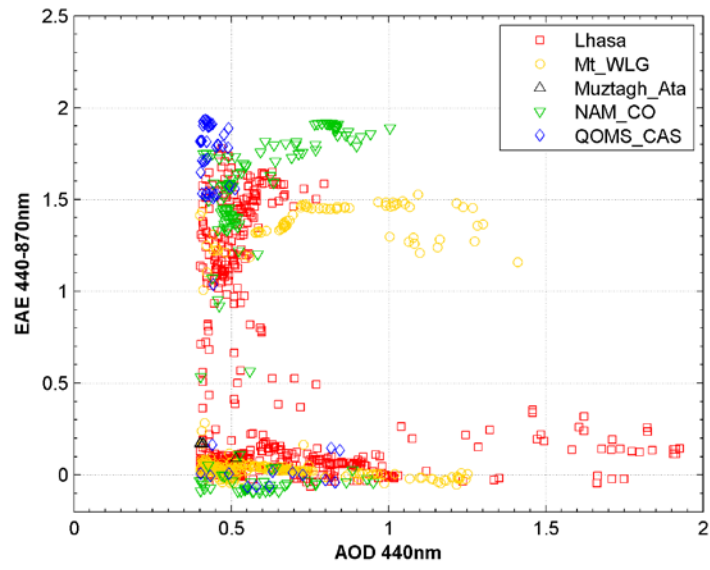
1  
2  
3

Figure 8. Trend of in the MODIS AOD at 550\_nm during 2006-2017.



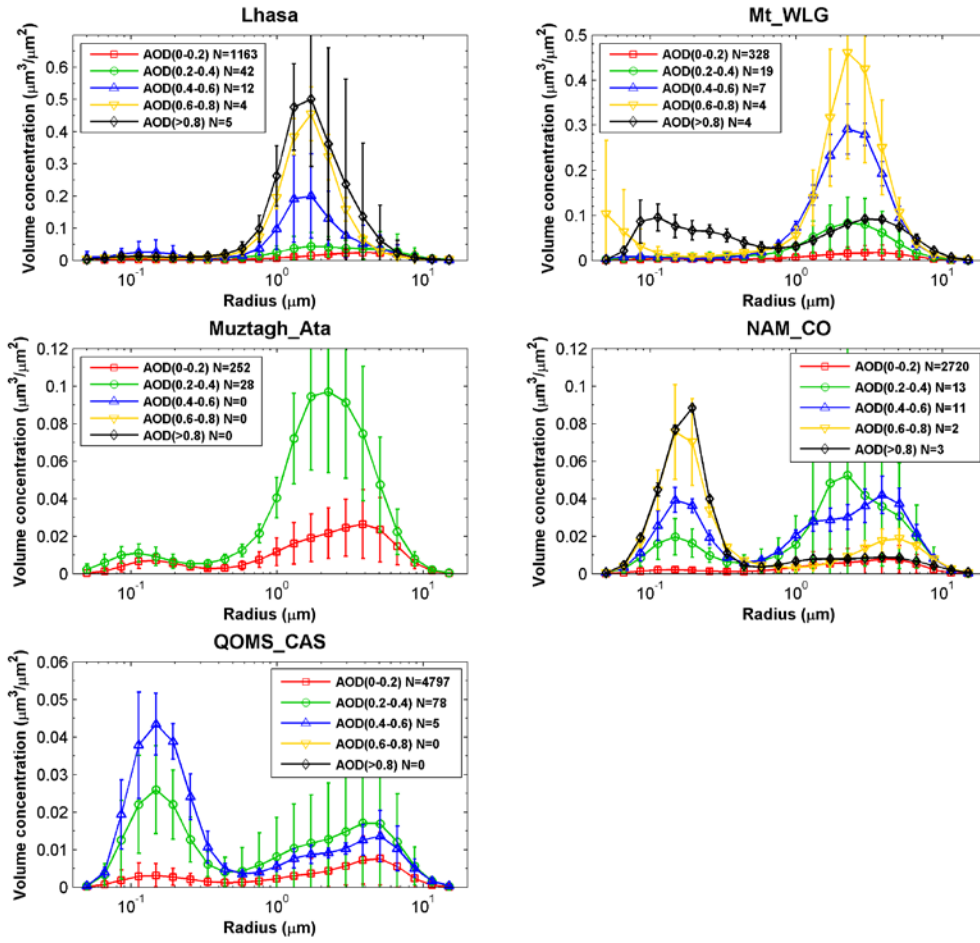
1  
2  
3

Figure 9. Trends of in the MODIS AOD at 550 nm during 2006-2017 in each season.



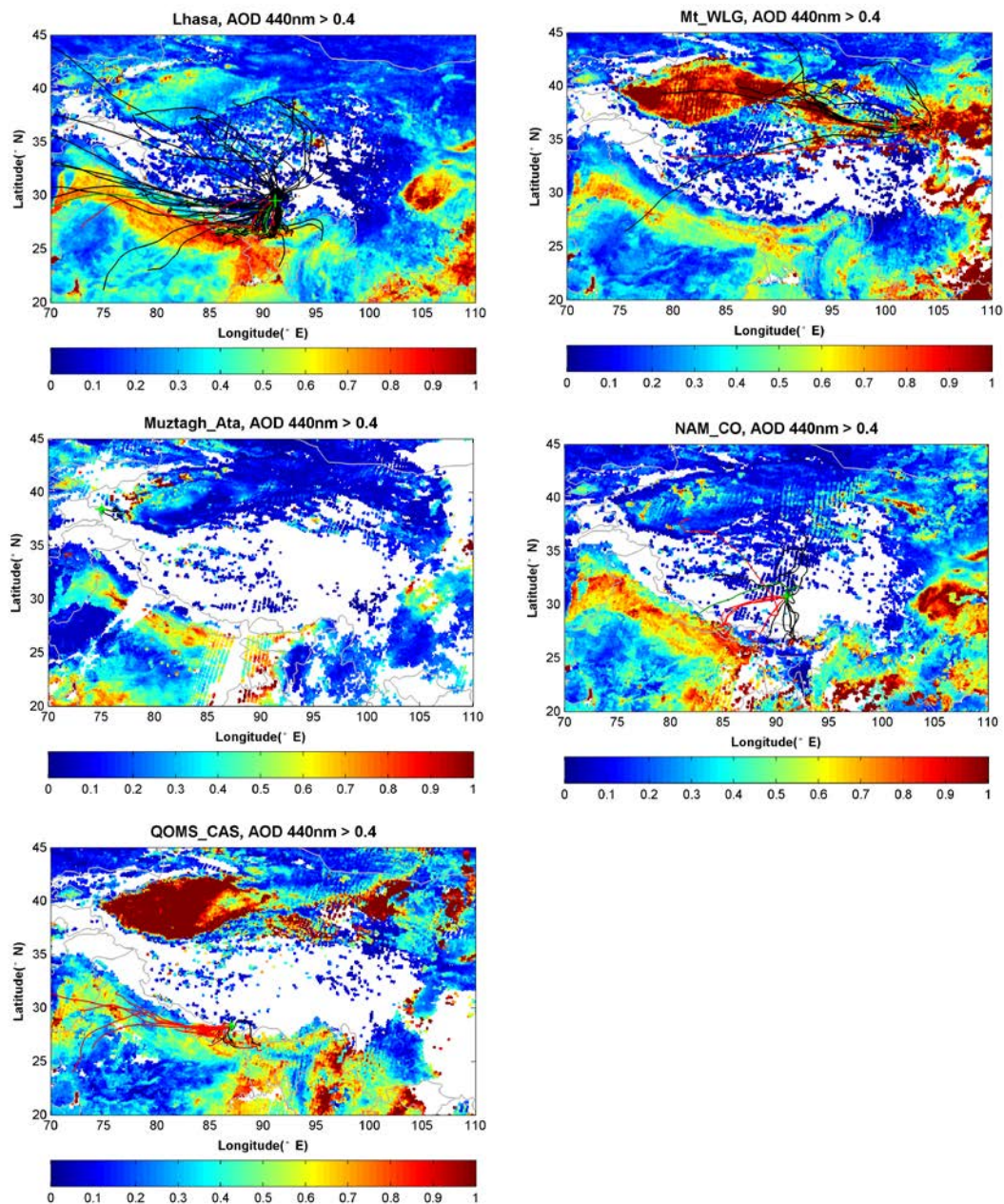
1  
2  
3  
4

Figure 10. AOD vs EAE (Only only CE318 AOD at 440\_nm > 0.4 is was considered) observed by CE318 at the five sites on the Tibetan plateau Plateau.



1  
2  
3  
4

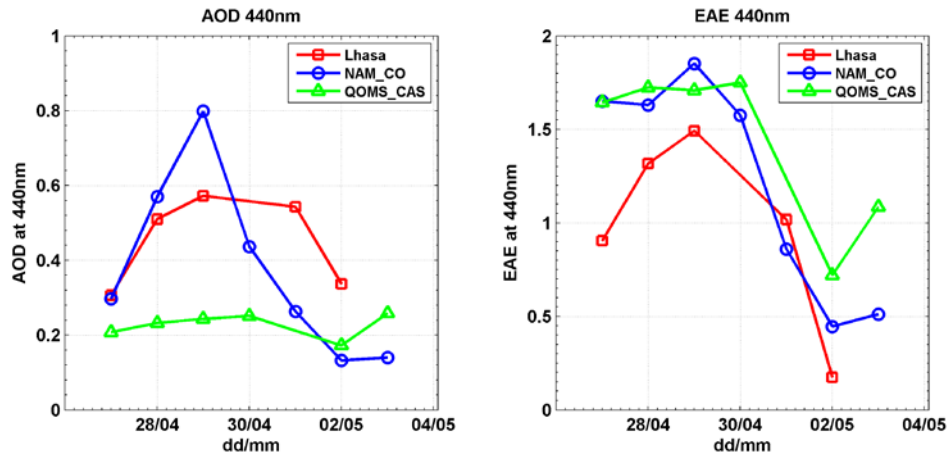
Figure 11. Aerosol size distribution binned by CE318 AOD at the five sites [on the Tibetan Plateau](#).



1

2 Figure 12. The back-trajectories ended at the five sites (10 m above ground level) on the TP overlaid  
 3 by with the mean MODIS C6 AOD at 550 nm on the aerosol pollution day observed by ground-based  
 4 CE318 (CE318 AOD >0.4). Red stands for EAE >1.0, black is for EAE <0.5, and green is for EAE  
 5 within 0.5-1.0.

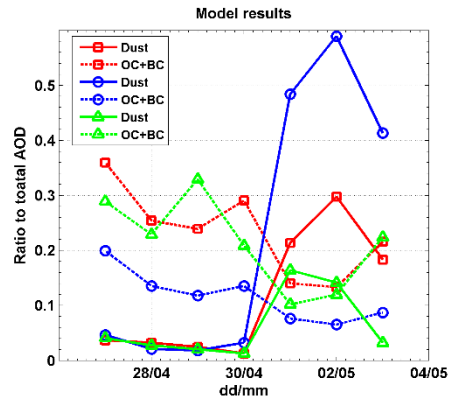
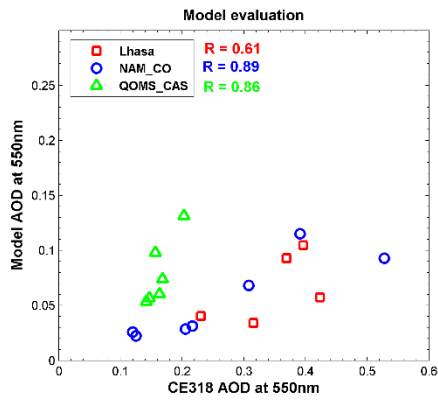
6



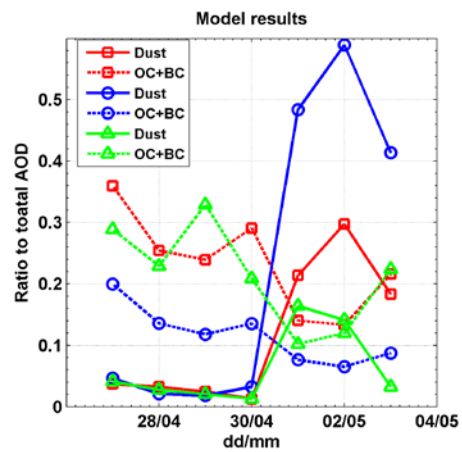
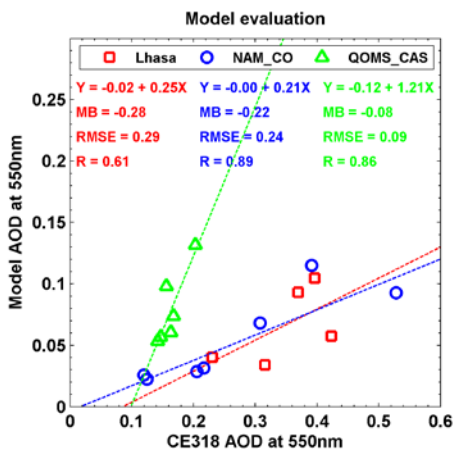
1

2 Figure 13. CE318 observed daily AOD at 440\_nm and EAE during 27April-27, 2016 – 3May-3, 2016 at  
 3 Lhasa, NAM\_CO and QOMS\_CAS.

4



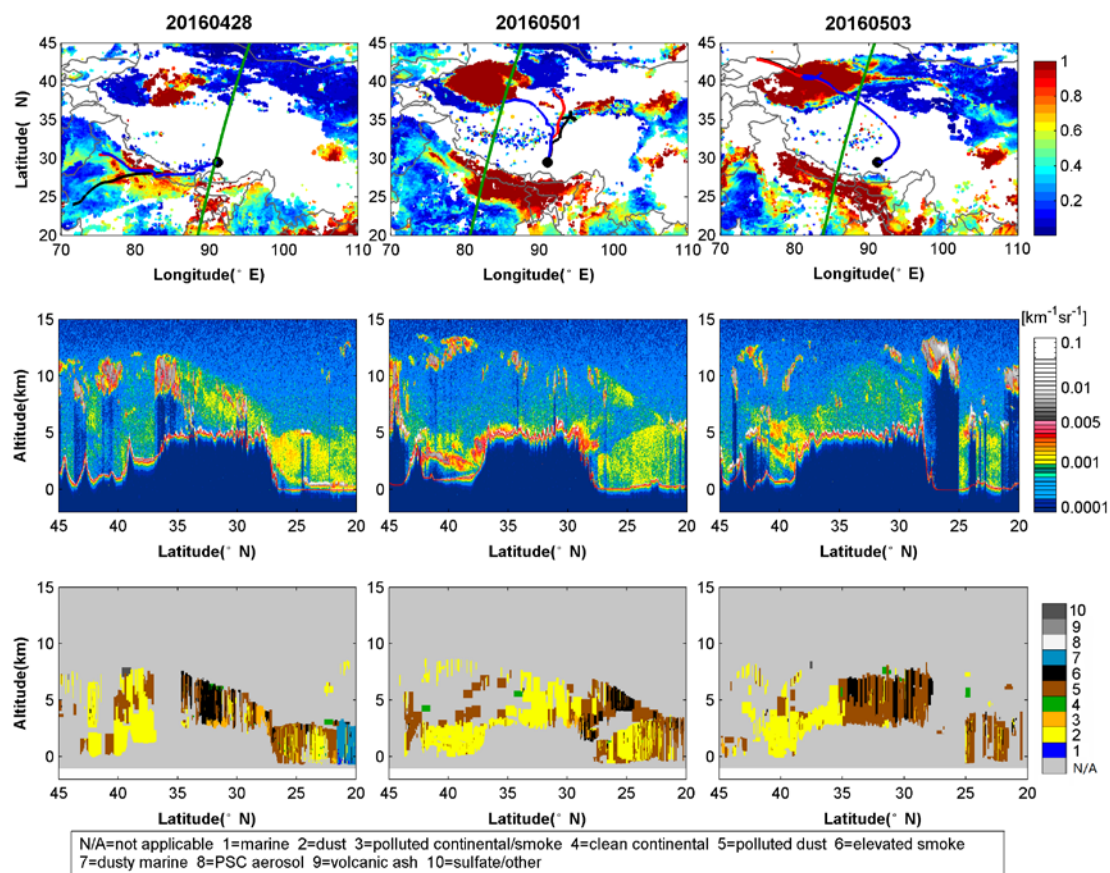
1



2

3 Figure 14. The GEOS-Chem model simulated the daily average AOD vs CE318 observed daily AOD at  
 4 550\_nm\_ and the ratios of dust or organic carbon (OC) and black carbon (BC) aerosol to the total AOD  
 5 during 27April-27, 2016 —3 May-3, 2016 at Lhasa, NAM\_CO and QOMS\_CAS. The statistical  
 6 parameters used in the modal evaluation are the same as those in Figure 5.

7



1  
2  
3  
4  
5  
6  
7

Figure 15. The MODIS C6 AOD at 550 nm and 72-hour back trajectories ended at Lhasa at three heights above the ground level (10 m in black, 500 m in red and 1000 m in blue lines) (the first row); the CALIOP-derived vertical profile of total attenuated backscatter at 532 nm (the second row); and the vertical feature mask of aerosol on 28 April, 1 May, and 3 May, 2016 over the ground track shown in the first row (green lines) (the third row).

1 Table 1. Site location and description.

| <b>Site name</b>   | <b>Lat(° N)</b> | <b>Lon(° E)</b> | <b>Site description, observation days and period</b>   |
|--------------------|-----------------|-----------------|--|
| <b>Lhasa</b>       | 29.50           | 91.13           | Urban station <del>over</del> <u>on</u> the Tibetan Plateau, 3648_m a.s.l., 1554 days, 2007.05~2017.12 |
| <b>Mt_WLG</b>      | 36.28           | 100.90          | Mountain, 3816 m a.s.l., 314 days, 2009.09~2013.07   |
| <b>Muztagh_Ata</b> | 38.41           | 75.04           | Mountain, 3674 m a.s.l., 84 days, 2011.06~2011.10  |
| <b>NAM_CO</b>      | 30.77           | 90.96           | Mountain, 4740 m a.s.l., 1061 days, 2006.08~2016.08  |
| <b>QOMS_CAS</b>    | 28.36           | 86.95           | Mountain, 4276 m a.s.l., 1623 days, 2009.10~2017.11  |

2

3

1 Table 2. Seasonal aerosol optical depth (AOD<sub>440nm</sub>) and extinction Angstrom exponent (EAE<sub>440-870nm</sub>) at  
 2 the five sites in [the](#) TP.

| Site               | AOD           |               |               |               | EAE           |               |               |               |
|--------------------|---------------|---------------|---------------|---------------|---------------|---------------|---------------|---------------|
|                    | MAM           | JJA           | SON           | DJF           | MAM           | JJA           | SON           | DJF           |
| <b>Lhasa</b>       | 0.16+0.<br>10 | 0.12+0.<br>08 | 0.10+0.<br>18 | 0.09+0.<br>08 | 0.72+0.<br>37 | 0.97+0.<br>40 | 1.11+0.<br>38 | 0.91+0.<br>52 |
| <b>Mt_WLG</b>      | 0.13+0.<br>16 | 0.14+0.<br>07 | 0.08+0.<br>11 | 0.08+0.<br>07 | 0.37+0.<br>38 | 0.65+0.<br>40 | 1.04+0.<br>80 | 0.58+0.<br>69 |
| <b>Muztagh_Ata</b> | NaN           | 0.14+0.<br>06 | 0.14+0.<br>05 | NaN           | NaN           | 0.73+0.<br>30 | 0.64+0.<br>27 | NaN           |
| <b>NAM_CO</b>      | 0.07+0.<br>07 | 0.06+0.<br>04 | 0.03+0.<br>05 | 0.03+0.<br>01 | 0.63+0.<br>44 | 0.62+0.<br>45 | 0.65+0.<br>32 | 0.78+0.<br>43 |
| <b>QOMS_CAS</b>    | 0.08+0.<br>06 | 0.06+0.<br>04 | 0.03+0.<br>01 | 0.03+0.<br>02 | 1.04+0.<br>38 | 0.76+0.<br>43 | 0.85+0.<br>51 | 1.10+0.<br>67 |

3  
4

1 Table 3. The percentages of EAE <0.5, 0.5-1.0, and >1.0 for high AOD observations at the five sites.

| Site               | N of AOD>0.4 | % EAE<0.5/N | % 0.5<EAE<1.0/N | % EAE>1.0/N |
|--------------------|--------------|-------------|-----------------|-------------|
| <b>Lhasa</b>       | 655          | 60.6        | 3.4             | 36.0        |
| <b>Mt_WLG</b>      | 290          | 73.4        | 0               | 26.6        |
| <b>Muztagh_Ata</b> | 5            | 100         | 0               | 0           |
| <b>NAM_CO</b>      | 140          | 27.9        | 2.8             | 69.3        |
| <b>QOMS_CAS</b>    | 59           | 23.7        | 0               | 76.3        |

2

3